Acta Geochim (2024) 43:638–660
https://doi.org/10.1007/s11631-023-00666-y

ORIGINAL ARTICLE

Features of sampling stream sediments of large river valleys under cryolithogenesis conditions in the Balygychan–Sugoy trough, North–East of Russia

Artem S. Makshakov[1] · Raisa G. Kravtsova[1]

Received: 24 July 2023 / Revised: 20 November 2023 / Accepted: 8 December 2023 / Published online: 4 January 2024

Abstract Comprehensive research has been implemented to raise the efficiency of the geochemical survey of stream sediments (SSs) that formed under the cryolithogenesis conditions. The authors analysed the composition, structure and specific features of the formation of exogenous anomalous geochemical fields (AGFs) identified through SSs of large river valleys of IV order. In our case, these were the valleys of Maly Ken, Ken and Tap Rivers. These rivers are located in the central and southern parts of the Balygychan–Sugoy trough enclosed in the Magadan region, North–East of Russia. The authors proposed a new technique to sample loose alluvium of SSs in the large river valleys along the profiles. The profiles were located across the valleys. The AGFs of Au, Ag, Pb, Zn, Sn, Bi, Mo and W were studied. Correlations between elements have been established. These elements are the main indicator elements of Au–Ag, Ag–Pb, Sn–Ag, Mo–W and Sn–W mineralization occurring on the sites under study. The results obtained were compared with the results of geochemical surveys of SSs. It is concluded that the AGFs recognized along the profiles reflect the composition and structure of eroded and drained ore zones, uncover completely and precisely the pattern of element distribution in loose sediments of large water flows. The alluvium fraction < 0.25 mm seems to be most significant in a practical sense, as it concentrated numerous ore elements. Sampling of this fraction in the river valleys of IV order does not cause any difficulty, for this kind of material is plentiful. The developed technique of alluvium sampling within large river valleys is efficient in searching for diverse mineralization at all stages of prognostic prospecting. It is applicable for geochemical survey of SSs performed at different scales both in the North–East of Russia, as well as other regions with similar climatic conditions, where the SSs are formed under the cryolithogenesis conditions.

Keywords Stream sediments · Large river valleys · Geochemical fields · Mineralization · Indicator elements · Geochemical survey

✉ Artem S. Makshakov
artem_m@mail.ru

[1] A.P. Vinogradov Institute of Geochemistry, Siberian Branch of the Russian Academy of Sciences, Favorskiy Str 1A, Irkutsk, Russia 664033

1 Introduction

It is evident that geochemical methods of prospecting are significant for regional forecasting and searching for ores. At the early stages of prospecting, it is highly efficient to employ a geochemical survey of stream sediments (SSs). These methods are primarily applied to assess vast areas at short time and at a low cost. The SSs were first used in prospecting ore deposits in the second half of the twentieth century. At the same time, geochemical methods through SSs were developed (e.g., Hawkes and Bloom 1956; Kvashnevskaya 1957; Boyle et al. 1958; Bogolyubov and Sochevanov 1959; Solovov 1959; Degrys 1961; Hawkes and Webb 1962; Polikarpochkin 1963; Dahlberg 1968; Bradshaw et al. 1972). Since then, they have been progressively upgraded and are still widely employed in exploration works. This evidence could be well exemplified by the recently published papers on this subject matter (e.g., Naseem et al. 2002; Ohta et al. 2005; Romanov 2008; Nude and Arhin 2009; Sokolov 2010; Yousefi et al. 2013; Zhang et al. 2013; Liu et al. 2014; Zuo 2014; Ali et al. 2015; Yilmaz et al. 2015, 2017, 2022; Chen et al. 2016; Shahrestani et al. 2018, 2019; Makshakov et al. 2019; Lin et al. 2020; Azmi et al. 2021; Makshakov and

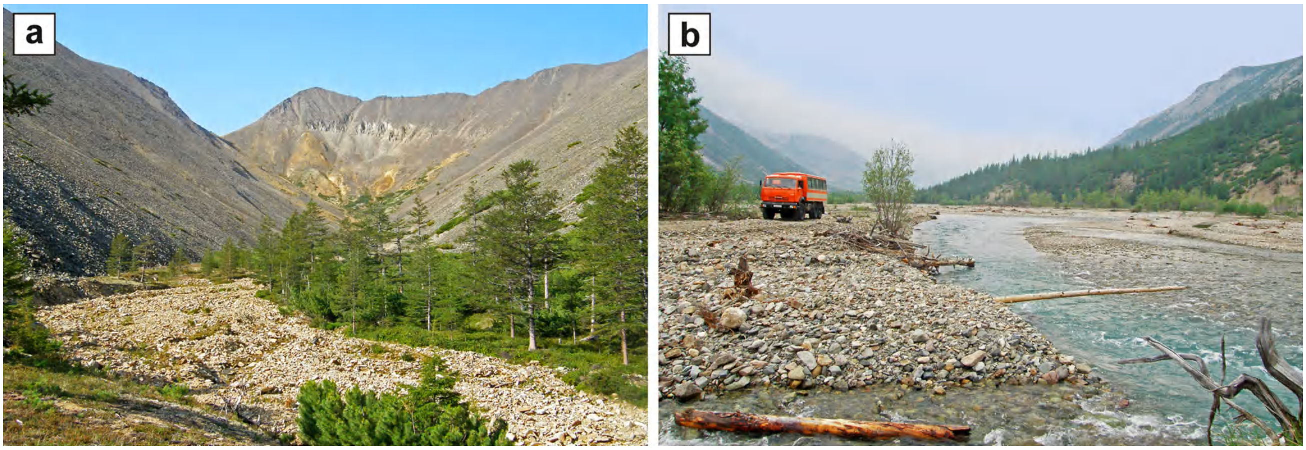

Fig. 1 Typical water flow valleys of I–II (**a**) and III–IV (**b**) orders, North–East of Russia

Kravtsova 2021; Ayari et al. 2022; Wang et al. 2022; Lipp et al. 2023; Marques et al. 2023).

All such papers deal mainly with the study of loose sediments (alluvium) of small water flows. Just these sediments are commonly sampled by prospectors in geochemical surveys of SSs. Such kinds of water flows are represented by small and large brooks extending for less than 10 km and running through the valleys of I–III orders (Horton 1945; Strahler 1952, 1957; Filosofov 1975; Kiryukhin and Shvets 2010) (Fig. 1a). Collecting samples is easy enough, for the valleys are normally less than 100 m wide. Following the method (Grigoryan et al. 1983), the samples are collected on the riverbed shallows of temporary and permanent water flows, at times on the flooded land, when the shallows are filled with water.

In contrast, researchers practically do not pay due attention to the loose sediments of larger water flows (small rivers extending for 10–50 km, running in the valleys of III–IV orders) (Fig. 1b). Such SSs are not often sampled. This is explained by the uncertainty in selecting sites for alluvium sampling, as due to lateral erosion the width of recent valleys of these rivers may achieve some hundred metres and even a few kilometres. In some locations in the valleys, the flood lands are boggy, the riverbed is uncertain, and the rivers are most often branching into numerous watercourses. In places, one can hardly locate the borders between the terraces above the flood land and flood land proper. Thus, considering the techniques applied in Russia (Polikarpochkin 1976; Grigoryan et al. 1983), it is recommended to execute sampling following two parallel routes running on both sides of the valley closely to the slopes. Practically, in geochemical surveys, sampling if present at all is performed mainly along the riverbed. Our research has shown that the enumerated techniques of sampling provide no results on discovering anomalies linked with mineralization. Therefore, it is vital to carry out comprehensive methodological work to investigate the SSs formed in large river valleys. The objective of this work is to develop the more effective technique of alluvium sampling in the river valleys of III–IV orders targeted to accurate identification of exogenous anomalous geochemical fields (AGFs) through SSs and, as a consequence, improvement of geochemical survey of SSs.

2 Characteristics of the study area

2.1 Geological background

The study of the SSs of large river valleys was carried out in the North–East of Russia (Magadan region) within the Okhotsk-Chukotka volcanogenic belt, incorporating the Balygychan–Sugoy trough (BST) (Fig. 2a). We have selected the sites on the Maly Ken and Ken Rivers in the centre (Fig. 2b), and Tap River in the south of the BST (Fig. 2c).

Two structural horizons participate in the geological setting of the central and southern parts of the BST. The lower horizon is composed of Triassic–Jurassic terrigenous sediments represented by sandstone, siltstone, argillite, tuff and coquina. All these rocks are exposed on the surface in mostly eroded southern part of the BST. The upper horizon is composed of Cretaceous terrigenous-volcanic rocks of the trough (Fig. 2b, c). On the study areas, the most ancient sediments of the BST are Early Cretaceous terrigenous coal-bearing rocks of the Omsukchan formation (K_1om). These rocks consist of sandstone, siltstone, argillite and conglomerate, and primarily occupy the BST centre. They are unconformably overlain by effusive rocks of the average composition of the Early-Late Cretaceous Tavatum formation (K*tv*). The formation is represented by andesite, andesite-basalt, their tuff, tuff-lava and dacite. The Late Cretaceous Nayakhan formation (K_2nh) of acidic volcanics is the youngest one in the trough. This sequence consists of rhyolite, rhyolitic

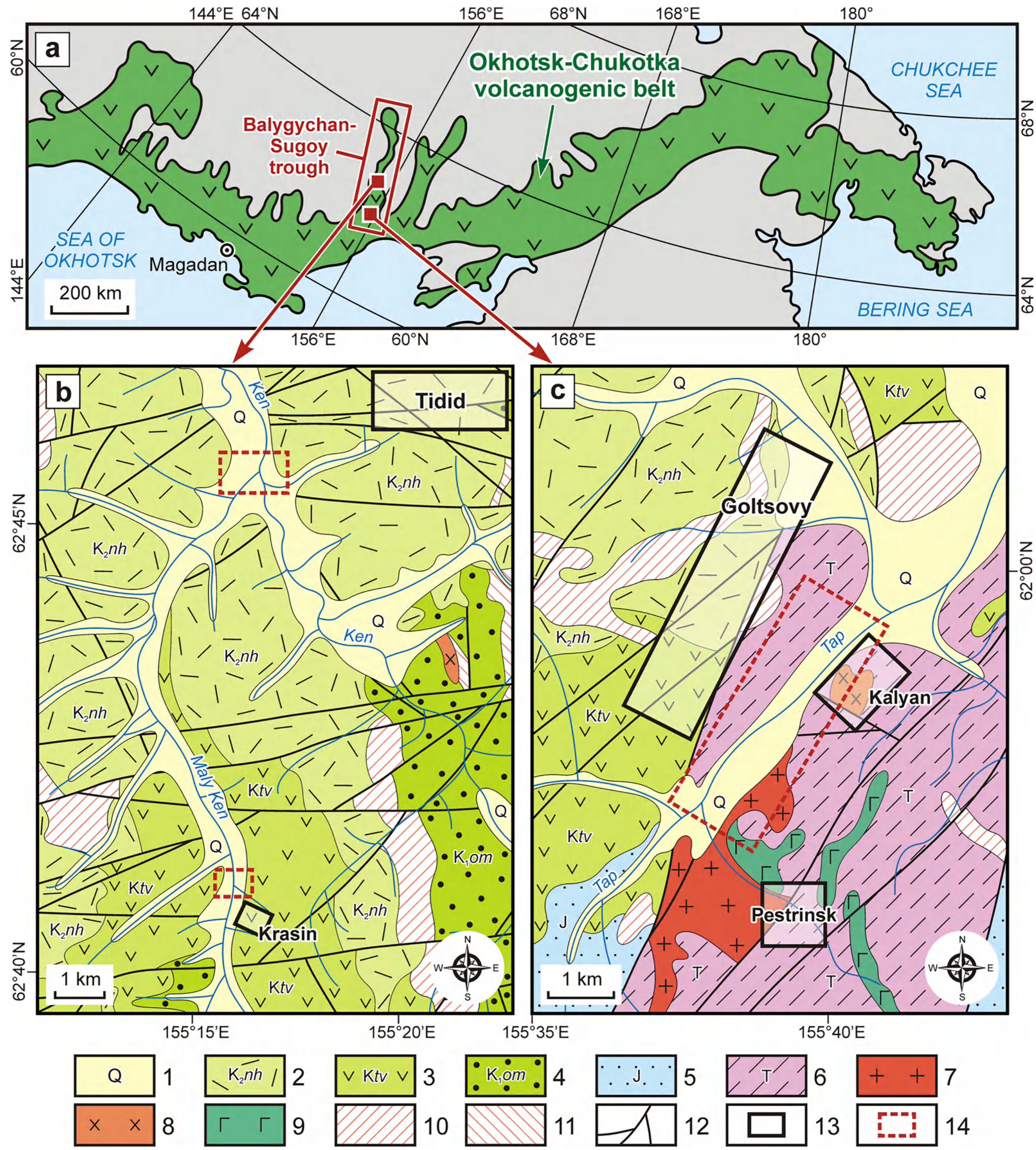

Fig. 2 Location of study area (**a**) and schematic geological maps of central (**b**) and southern (**c**) parts of the BST. The images were constructed using materials from geological funds and the Dukat Geological Survey, with additions and modifications after (Struzhkov and Konstantinov 2005; Belyi 2008). 1. Quaternary sediments (Q); 2. Late Cretaceous rhyolite, rhyolitic ignimbrite and tuff and rhyodacite (Nayakhan formation, K_2nh); 3. Early-Late Cretaceous andesite, andesite-basalt, their tuff and tuff-lava and dacite (Tavatum formation, K*tv*); 4. Early Cretaceous sandstone, siltstone, argillite, conglomerate and coal seams (Omsukchan formation, K_1om); 5. Jurassic sandstone, siltstone and argillite (J); 6. Triassic sandstone, siltstone, argillite, tuff, calcareous sandstone and coquina (T); 7–9. Late Cretaceous intrusions: 7. leucogranite, 8. diorite and 9. gabbro-diorite; 10 and 11. subvolcanic rocks: 10. Late Cretaceous rhyolite and nevadite and 11. Early Cretaceous rhyolite; 12. faults; 13. sites of deposits and prospects; 14.sites to study SSs of large river valleys

ignimbrite and tuff and rhyodacite. The intrusive rocks are spread widely as Late Cretaceous leucogranite and hypabyssal subvolcanic bodies of rhyolite, in places nevadite. The intrusions of Late Cretaceous diorite and gabbro-diorite, as well as Early Cretaceous subvolcanic bodies of rhyolite occur occasionally. The detailed structural, geological and metallogenic characteristics of the study area have been described in a great many works (e.g., Goncharov et al. 1984; Rodnov and Zaytsev 1985; Umitbaev 1986; Tauson et al. 1990; Konstantinov et al. 1993, 1998, 2003; Kravtsova et al. 1996, 2003; Kuznetsov and Livach 2005; Struzhkov and Konstantinov 2005; Belyi 2008; Sidorov et al. 2009, 2011; Kravtsova 2010; Volkov et al. 2018; Livach and Tretyakova 2022).

2.2 Types of mineralization

The survey sites enclose gold–silver (*Au–Ag*), silver–polymetallic (*Ag–Pb*), tin–silver (*Sn–Ag*), tin–rare metal (*Sn–W*) and rare metal (*Mo–W*) deposits and prospects (Fig. 2b,c).

The *Au–Ag* mineralization is available at the Krasin prospect (Fig. 2b). The lower-ore intervals mainly approach the surface, particularly at the stream-drained sites. The data of the Dukat Geological Survey indicate that the ore bodies occur within the mineralized zone of breaking in essentially silicified and kaolinized Early-Late Cretaceous andesite of the Tavatum formation cut by the dykes and small stocks of granodiorite porphyry of the same age. Ores consist of the veins and linear zones of veinlets with impregnated, nest- and streak-like distribution of sulphides. The veins and veinlets have quartz-carbonate and quartz-feldspar-carbonate compositions. The most widespread ore minerals are pyrite, rarely sphalerite; chalcopyrite, galena and pyrrhotite are even less common. Out of Ag minerals, argentite and pyrargyrite predominate. In some cases, proustite, polybasite, stromeyerite and native Au and Ag are found. Gold is present as kustelite and electrum. Its larger part as fine-dispersed particles are enclosed in pyrite, which is the main ore mineral. The pyrite amount (together with sphalerite) in ores increases at depth up to 10%. The geochemical composition of ores is typical for the lower-ore intervals of *Au–Ag* deposits in the BST (Kravtsova and Zakharov 1996; Kravtsova et al. 2003; Kravtsova 2010). High contents are typical for Ag, Sb and Zn, with fewer high contents for Au, As, Cu, B and Pb and low contents for Hg.

The *Ag–Pb* ores are discovered at the Tidid (Fig. 2b) and Goltsovy (Fig. 2c) deposits.

At the Tidid deposit, ore bodies have a subbedded form and are represented by veins, veinlet zones and veined-disseminated mineralization in stratified coaly-terrigenous Early Cretaceous sediments of the Omsukchan formation, in places in Late Cretaceous rhyolite of the Nayakhan formation or on their contact. The composition of ores varies from essential sulphide on the surface to sulphide-quartz at the middle horizon and chlorite-quartz at lower horizons. The veins and veinlets are largely composed of quartz, orthoclase and chlorite, as well as later carbonate. The most common ore minerals represent galena, sphalerite, chalcopyrite, arsenopyrite and silver minerals (freibergite, pyrargyrite and stephanite). Not so abundant are pyrite, pyrrhotite, boulangerite, marcasite, stannite, miargyrite, diaphorite, acanthite, polybasite and native silver (Shilo et al. 1992; Plyashkevich 2002; Konstantinov et al. 2003; Kravtsova 2010; Savva 2018).

Ores of the Goltsovy deposit are zones of veined-impregnated mineralization, in places extensive veins and lenses in rhyolite of the Nayakhan formation (Late Cretaceous). Ore bodies consist of quartz, carbonates, hydromica and sericite, rarely chlorite, kaolinite and adularia. Ore minerals are mainly galena, sphalerite and freibergite. To add, the ores are also typified by pyrargyrite, tetrahedrite, polybasite, miargyrite, stephanite, native Ag, boulangerite, acanthite, pyrite and pyrrhotite. The minerals like sternbergite, chalcopyrite, stannite, cassiterite, arsenopyrite, magnetite and hematite are found quite infrequently. Diaphorite and gudmundite occur even more seldom (Shilo et al. 1992; Konstantinov et al. 1993, 2003; Kravtsova et al. 1996, 1998; Plyashkevich 2002; Struzhkov and Konstantinov 2005; Kravtsova 2010; Savva 2018; Savva et al. 2021).

High contents in *Ag–Pb* ores are typical for Ag, Pb, As and Sb, a bit lower one for B, Zn, Hg and Sn, low values of Cu and Bi. The occurrence of Sn and Bi is linked with the *Sn–Ag* mineralization, which is generally combined with *Ag–Pb* ones (Tauson et al. 1990; Kravtsova et al. 1996; Kravtsova 2010).

Sn–Ag mineralization occurs at deep horizons and on the southeastern flanks of the Goltsovy deposit. Ores are represented by veined-impregnated and impregnated linear zones in Late Cretaceous volcanics of mainly rhyodacite composition of the Nayakhan formation. The gangue minerals are quartz, chlorite, calcite and sericite. They may also show biotite and tourmaline, infrequently, however. The main ore minerals are sphalerite, argentite, galena, stannite, chalcopyrite, tennantite, tetrahedrite, As-pyrite and pyrrhotite. Cassiterite, arsenopyrite and native Ag are rare (Kravtsova et al. 1996, 1998; Kravtsova 2010). Ores show high concentrations of Ag, Sn, As and Sb, and not so high Bi, Zn, Pb, Cu and B (Tauson et al. 1990; Kravtsova et al. 1996; Kravtsova 2010).

Sn–W and *Mo–W* mineralization was recognized in the unprofitable Kalyan and Pestrinsk prospects, respectively (Fig. 2c). These types of mineralization are related to Late Cretaceous granitoids. The processes of their greisenization (stockworks and veining areas) and hornfelsing proceeded broadly. Greisens are located in the roof of massifs. Hornstones developed both within the granitoids and within the

Triassic host terrigenous rocks. The main gangue minerals are quartz, biotite, feldspars and muscovite, smaller amounts of apatite, fluorite, carbonates and chlorites. Besides, there are pyroxenes, amphiboles, tourmaline, beryl and topaz. The main ore minerals are scheelite, molybdenite, pyrite, wolframite and pyrrhotite. Arsenopyrite, cassiterite, chalcopyrite, magnetite and hematite are rarely found; sphalerite and galena are available only in single cases (Kravtsova et al. 1996; Kravtsova 2010). *Sn–W* and *Mo–W* mineralization is characterized by high contents of W, As and Bi, not so high of Sn and Mo, low of B, Zn, Cu, Pb and Ag (Tauson et al. 1990; Kravtsova et al. 1996; Kravtsova 2010).

2.3 Topographic and climatic features

The Omsukchan ridge is the major mountainous unit lying between the Balygychan and Sugoy Rivers (Kolyma River tributaries). In the south of the BST, the ridge makes the Kolyma–Okhotsk watershed. The relief resembles the Alpine type. The maximal heights of peaks are about 1000 to 1700 m. The peaks look roundish or acute. The slope gradient reaches 30°, at the foot up to 45°.

The mountainous slopes and peaks are covered with large boulders of eluvium and deluvium about 3–5 m thick. The foothills are covered with thick sediments of colluvium. The exposure of bedrock is mainly poor.

This region is characterized by a sharply continental climate. Precipitation is irregular, and it is mostly rain in summertime. In summer, the water temperature of streams and rivers is never above 4–5 °C; in winter, most streams and small rivers freeze completely. The snow cover forms in September and completely melts in June. Cryolithogenesis conditions are omnipresent.

The main local watercourses are the Ken, Maly Ken and Tap Rivers. They belong to the Kolyma and Viliga river basins. Following the existing classification (Horton 1945; Strahler 1952, 1957; Filosofov 1975; Kiryukhin and Shvets 2010), the valleys of these rivers may be attributed to IV order, as they extend for 18–45 km and are formed by the confluence of stream valleys of III order. Closer to the source, the river valleys undergo intense deep and lateral erosion and have a V-shaped cross profile. In the middle and lower reaches, the valleys undergo lateral erosion, they begin to accumulate sediments, and their cross profile becomes the trough-like.

Regional geography, climate, drainage system and flora are described in detail in (Livach et al. 2007a, b).

3 Materials and methods

3.1 Geochemical sampling

The materials for the study were samples of alluvial sediments collected in the valleys of Maly Ken, Ken and Tap Rivers (Fig. 2). Samples were taken along profiles located across the river valleys below the mouths of the streams falling into them (Fig. 3). The streams themselves drain mineralization. The profiles extended from 110 to 560 m depending on the valley width. Alluvium was sampled from the surface in the direction from one side of the valley to another. The sampling points were spaced within 5–30 m (on average about 20 m). Mainly sandy, sandy silt and less frequently sandy gravel material were sampled. Preference was given to the sandy silt fraction, which generally prevails in the valleys of the IV order. The sample weight was 400–500 g. They were thoroughly dried and sieved into two fractions: usually accepted for prospecting <1 mm (common) and less traditional <0.25 mm (fine). The fractions were mechanically grated in steel glasses on a vibrating grinder to the state of powder (~200 mesh). The locations of the alluvium samples are shown in Fig. 3. The total number of samples in the valleys of Maly Ken, Ken and Tap Rivers was 17, 18 and 90, respectively.

3.2 Sample analysis

We studied the composition, structure and specific features of formation of the AGFs of Au, Ag, Pb, Zn, Sn, Bi, Mo and W, which are the main indicator elements of *Au–Ag*, *Ag–Pb*, *Sn–Ag*, *Mo–W* and *Sn–W* types of mineralization occurring at the study sites. The element contents in alluvium samples were determined at the chemical laboratories of the Institute of Geochemistry, Siberian Branch of the Russian Academy of Sciences (IGC SB RAS), Irkutsk, Russia.

First, all the samples were analysed through a spectral semi-quantitative atomic-emission analysis (SSA) for a wide range of elements (Raykhbaum 1976). In this technique, the sample powders were blown-and-spilled into the AC arc on a Russian spectral device. It included DFS-8 spectrograph, USA-5 attachment and DG-2 generator. The spectra were visually interpreted using DSP-1 spectral projector. Analysed by Valentina Kishechnikova.

The results of the SSA were verified through a quantitative atomic-emission analysis (Vasileva and Shabanova 2012). A Russian spectral facility was applied, including a DFS-458S spectrograph, an automated device to introduce samples into electric arc with an inbuilt spectral analytical generator, and a multi-channel analyser of atomic emission spectra. Analysed by Irina Vasileva and Elena Shabanova.

Gold contents in samples were determined through an atomic-absorption spectrometry (AAS) according to method

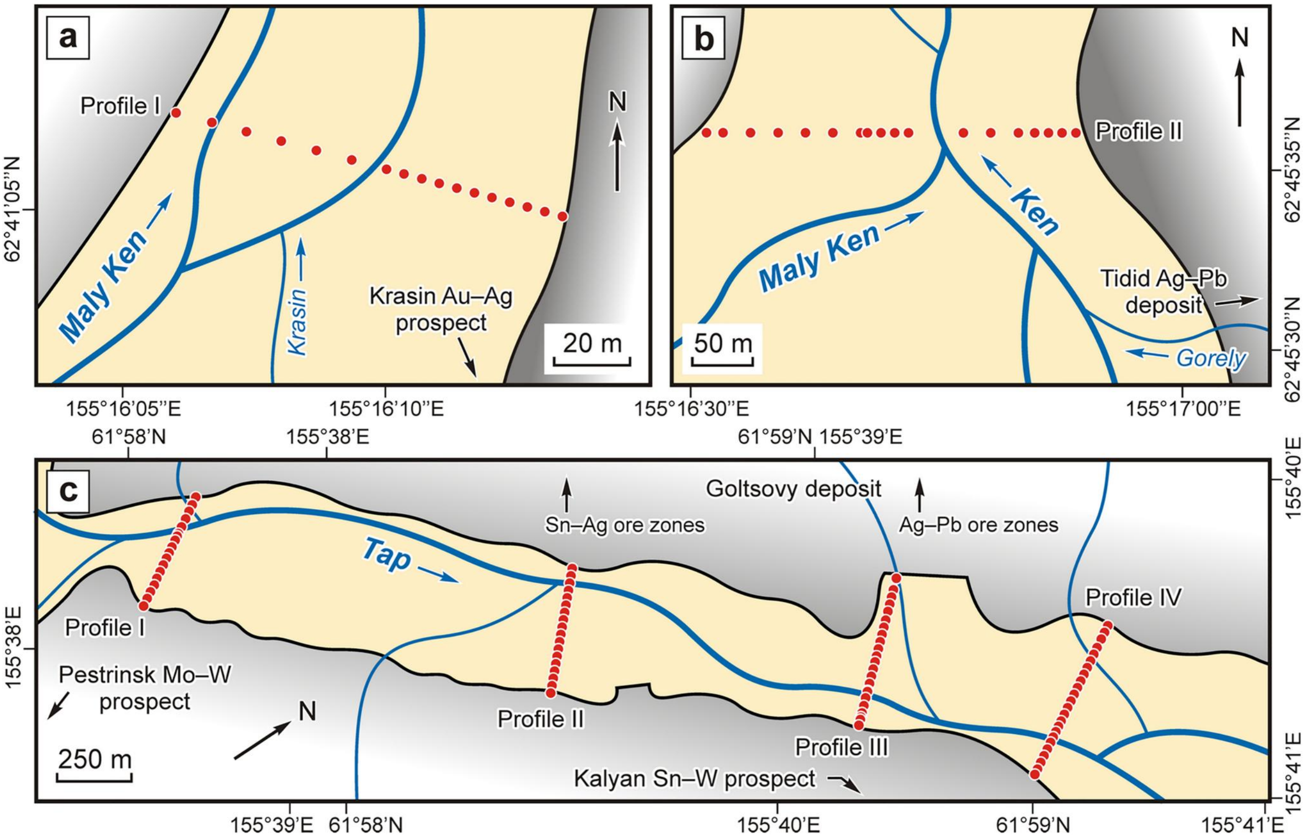

Fig. 3 The locations of alluvium samples in investigating SSs in the Maly Ken (**a**), Ken (**b**) and Tap (**c**) River valleys

(Torgov and Khlebnikova 1977; Rogozhin 2016). Samples were pre-decomposed with a mixture of acids. Gold was extracted with organic sulphide solution. Perkin-Elmer M-303 and M-503 (USA) spectrometers with an HGA-72 graphite atomizing furnace from the same company were used. Analysed by Pavlina Dolgikh, Tamara Krasnoschekova and Valentina Vlasova.

3.3 Data processing

Golden Software Surfer (USA) and Microsoft Office Excel (USA) software we applied to the analytical data processing, to plotting preliminary schemes of element distribution and to obtain diverse statistical data.

The method of multidimensional fields (Kitaev 1990) to study of structure and composition of the AGFs identified through SS we used; it is also used in plotting geochemical maps. This method uses automatic classification to differentiate the analytical data into the system of like quantities. It reveals frequently available combinations of elements with close quantitative values. As a result, AGFs of each element were plotted.

During the study of AGFs, exogenous ones inclusive, an important role was given to selection of the background content (C_b) for each element. In this paper, the authors accepted the C_b calculated through the 40–50 % level of the accumulated frequency ratio of element contents (40–50 % fractile of distribution) in SSs. In calculating C_b, large amounts of analytical data (for > 3000 samples) were employed. This data amounts were obtained previously when performing geochemical survey of SSs at a 1:50 000 scale within the central and southern segments of the BST. Table 1 shows the C_b we used for the elements, the AGFs of which are discussed in this paper.

4 Results

4.1 Geochemical fields identified through SSs of the Maly Ken and Ken Rivers

To study the exogenous AGFs in the Maly Ken and Ken River valleys two profiles were placed within the centre of the BST. We have analysed the composition and structure of geochemical fields of Au, Ag, Pb and Zn, the main indicator elements of *Au–Ag* and *Ag–Pb* types of mineralization. Profile I was located in the Maly Ken River valley below the mouth of the Krasin stream draining the *Au–Ag* prospect of

Table 1 The background contents accepted in the paper for main indicator elements of mineralization versus average contents of elements in different rocks (ppm)

Element	C_b	C_{av} (Vinogradov 1962)	C_{ac} (Vinogradov 1962)	C_{Ec}	
				(Vinogradov 1962)	Taylor (1964)
Au	0.002	–	0.0045	0.0043	0.004
Ag	0.1	0.07	0.05	0.07	0.07
Pb	20	15	20	16	12.5
Zn	50	72	60	83	70
Mo	2	0.9	1	1.1	1.5
W	1	1	1.5	1.3	1.5
Sn	4	–	3	2.5	2
Bi	0.1	0.01	0.01	0.009	0.17

C_b, accepted background contents; C_{av}, in average rocks; C_{ac}, in acidic rocks; C_{Ec}, in the Earth's crust. Dash (–), no data. The background content of Bi is conventionally accepted with regard to detection limit of this element (0.04 ppm) in AAS method

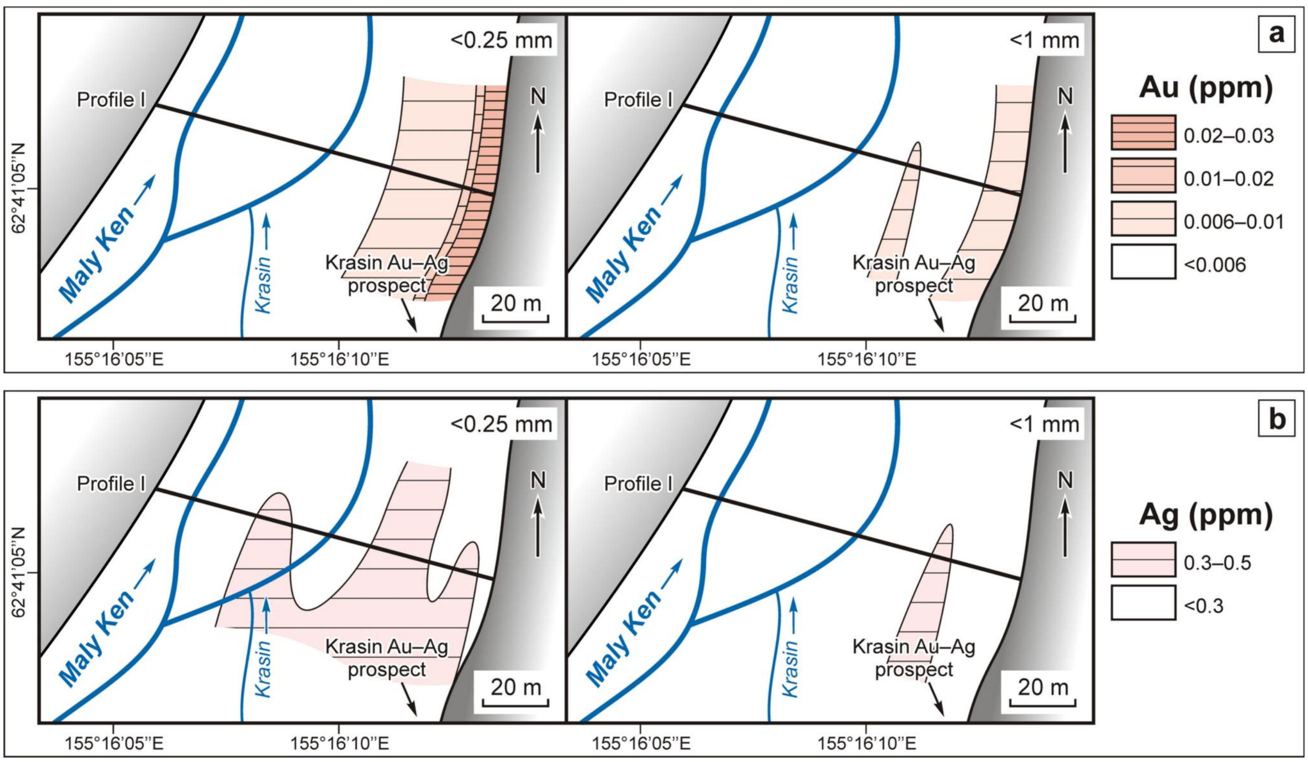

Fig. 4 The Au (**a**) and Ag (**b**) AGFs identified through SSs in Maly Ken River valley (profile I). Fractions < 0.25 mm and < 1 mm

the same name (Figs. 2b, 3a). Profile II was placed in the Ken River valley below the Maly Ken River mouth, after the Gorely stream inflow (right tributary of Ken River) draining the Tidid *Ag–Pb* deposit (Figs. 2b, 3b).

In *profile I*, we explored the AGFs of Au and Ag (Fig. 4). The anomalous concentrations of these elements were determined in the two fractions of alluvium. The largest AGFs were located by analysing the fine fraction, which displayed moreover maximum contents of Au, e.g., 0.01–0.03 ppm. The contrast ratios (CR[1]) of Au in the AGFs varied from 5 to 15. The Ag contents reached values of 0.3–0.5 ppm at CR = 3–5. These fields of Au and Ag were identified on the right side of the Maly Ken River valley, closer to the confluence of the Krasin stream. Further, towards the central part of the valley and its left side, the Au and Ag contents

[1] CR is the number obtained by dividing the average element content in the AGF by its background.

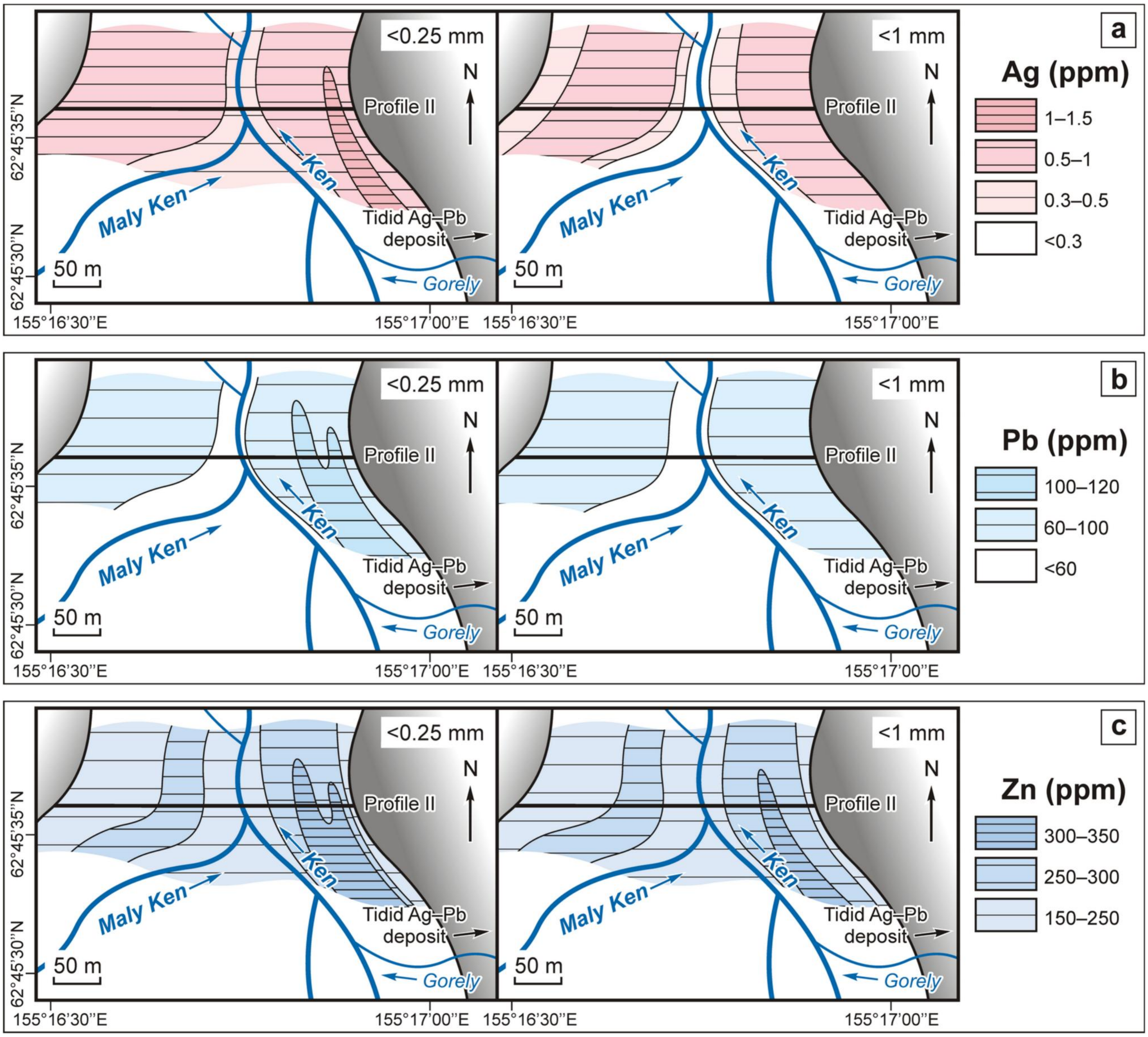

Fig. 5 The Ag (**a**), Pb (**b**) and Zn (**c**) AGFs identified through SSs in Ken River valley (profile II). Fractions < 0.25 mm and < 1 mm

in SSs gradually decreased to near-background values (Au < 0.006 ppm at CR < 3 and Ag < 0.3 ppm at CR < 3). In the common fraction of alluvium, the Au contents did not exceed 0.01 ppm at CR < 5 (Fig. 4a). Like in the fine fraction, the Ag contents in the common fraction reached values of 0.3–0.5 ppm at CR = 3–5 (Fig. 4b). The same pattern was observed in the distribution of Au and Ag AGFs, as in the fine fraction. They were also located closer to the right side of the Maly Ken River valley.

The correlation analysis revealed only a weak relationship between Au and Ag. In the fine and common fractions of alluvium, the pair correlation coefficients were + 0.26 and + 0.20, respectively (the sample size in both cases was 17).

In *profile II*, we explored the AGFs of Ag, Pb and Zn (Fig. 5). The anomalous concentrations of these elements were determined in all two fractions of alluvium, but in this respect, mostly representative was fraction < 0.25 mm. This particularly concerns the AGFs of Ag (Fig. 5a) and Pb (Fig. 5b). The fine fraction was found to contain maximum concentrations of these elements: Ag to 1–1.5 ppm (CR = 10–15), Pb to 100–120 ppm (CR = 5–6). All these anomalies were identified closer to the right side of the valley, the place of the Gorely stream confluence. In the direction to the left side of the valley, particularly in the mouth of the Maly Ken and Ken Rivers the element contents noticeably decreased: Ag to 0.3–1 ppm (CR = 3–10), Pb to 60–100 ppm and less (CR = 3–5 and less). In the common fraction the Ag and Pb contents turned to be lower: 0.3–1 ppm and less (CR = 3–10 and below) and 60–100 ppm and less (CR = 3–5 and less), respectively (Fig. 5a, b). These element concentrations were identified both for the left and right valley sides.

The Zn contents in profile II in both fractions reached 300–350 ppm at CR = 6–7 (Fig. 5c). The Zn AGFs with such contents, same as the most contrasting Ag and Pb anomalies, were also located closer to the right side of the valley. In the direction to the central part (the mouth of Maly Ken and Ken Rivers) and left side of the valley the element contents decreased to 150–250 ppm (CR = 3–5).

Correlation analysis confirmed the relationships between Ag, Pb and Zn. In the common alluvium fraction, Ag–Pb (+ 0.73) exhibited strong relationship, and Pb–Zn (+ 0.52) and Ag–Zn (+ 0.37) had moderate relationships (sample size was 18). In the fine fraction, moderate relationships were established for Ag–Pb (+ 0.55) and Pb–Zn (+ 0.55), while Ag–Zn had a weak relationship (+ 0.23) (sample size was 18).

4.2 Geochemical fields identified through SSs of the Tap River

The study of exogenous AGFs in the Tap River valley was performed along four profiles located within the southern part of the BST and oriented across the valley. We have analysed the composition and structure of geochemical fields of Ag, Pb, Zn, Sn, Bi, Mo and W, which are the main indicator elements *Ag–Pb*, *Sn–Ag*, *Sn–W* and *Mo–W* types of mineralization. On the left side of the valley, on its slopes, there are *Ag–Pb* and *Sn–Ag* ore zones of the Goltsovy deposit, on the right side there are *Sn–W* and *Mo–W* prospects Kalyan and Pestrinsk, respectively (Figs. 2c, 3c).

Silver and *lead* had anomalous concentrations in all fractions of alluvium of the Tap River (Fig. 6a, b). The Ag contents in AGFs varied from < 0.3 ppm (CR < 3) to 6 ppm (CR = 60), the Pb contents from < 60 ppm (CR < 3) to 300 ppm (CR = 15). Maximal concentrations of Ag (4–6 ppm, CR = 40–60) and Pb (200–300 ppm, CR = 10–15) were identified in the fine fraction. In the common fraction, they did not exceed of 2–4 ppm (CR = 20–40) for Ag and 100–200 ppm (CR = 5–10) for Pb (Fig. 6a, b).

The most contrasting AGFs of Ag and Pb with contents 1–6 ppm (CR = 10–60) and 100–300 ppm (CR = 5–15), respectively, were detected in profiles III and IV in all fractions of alluvium. They were occurred on the left side of the Tap River valley, where in the watershed area the *Ag–Pb* ore zones of the Goltsovy deposit are located. The element concentrations gradually decreased upstream from profile III along the left side of the valley, at the site of influence of small tributaries draining *Sn–Ag* ore zones of the Goltsovy deposit (profiles I and II). In this area, the fields of lower contrast were identified: Ag–0.3–1 ppm at CR = 3–10, Pb–60–100 ppm at CR = 3–5.

On the right side of the valley, the contents of these elements were found to be minimal. The near background contents of Ag (< 0.3 ppm, CR < 3) and Pb (< 60 ppm, CR < 3) were revealed in profiles I and II, at the influence area of small water flows draining the *Mo–W* Pestrinsk prospect. The Ag contents in AGFs did not exceed 1 ppm (CR < 10), Pb contents 100 ppm (CR < 5) in profiles III and IV, at the influence area of small water flows draining the *Sn–W* Kalyan prospect.

Zinc, in comparison with Ag and Pb, in alluvium of the Tap River had only low contents. They varied from < 150 ppm (CR < 3) to 500 ppm (CR = 10) (Fig. 6c). Mostly contrasting AGFs of Zn with contents 250–500 ppm (CR = 5–10) identified only in the fine fraction of alluvium and only in profiles III and IV. These anomalies extended on the left side of the Tap River valley from profile III, below the sites of *Ag–Pb* ore zones of the Goltsovy deposit, downstream to the central part of the valley through profile IV. They were also discovered on the right side of the valley in profile IV, where the *Sn–W* mineralization (Kalyan prospect) appears on the slopes. The less contrasting fields with contents 150–250 ppm (CR = 3–5) were discovered on the left side of the valley in profile II, where the *Sn–Ag* mineralization (southwestern flank of the Goltsovy deposit) is available on the slopes. Further upstream in the direction to profile I, the Zn contents gradually decreased and became near-background (< 150 ppm, CR < 3). In the common fraction, the Zn concentrations did not exceed of 150–250 ppm (CR = 3–5) (Fig. 6c). The anomalies with these contents were located only in profiles II–IV. They extended along the left side of the valley from influence area of *Sn–Ag* and *Ag–Pb* ore zones of the Goltsovy deposit.

Tin and *bismuth* in SSs of the Tap River formed quite contrasting AGFs. The anomalous concentrations of these elements were found in all two alluvium fractions and in all profiles (Fig. 7). The Sn contents in AGFs varied from < 12 ppm (CR < 3) to 160 ppm (CR = 40), Bi contents from < 0.3 ppm (CR < 3) to 5 ppm (CR = 50). The highest concentrations of Sn (40–160 ppm, CR = 10–40) and Bi (4–5 ppm, CR = 40–50) were determined in the fine fraction. In the common fraction of alluvium, Sn concentrations did not exceed 20–40 ppm at CR = 5–10 (Fig. 7a). The Bi contents reduced slightly to 3–4 ppm at CR = 30–40 (Fig. 7b).

The most contrasting anomalous fields of Sn with the contents 100–160 ppm (CR = 25–40) (Fig. 7a) were found only in profile II along the left valley side, its slopes hosting *Sn–Ag* ore zones of the Goltsovy deposit. The AGFs with the lower Sn contents (40–100 ppm, CR = 10–25) occupied a larger area within the valley. They extended from profile II along the left valley side downstream to profile IV. The AGFs with the same contents were also

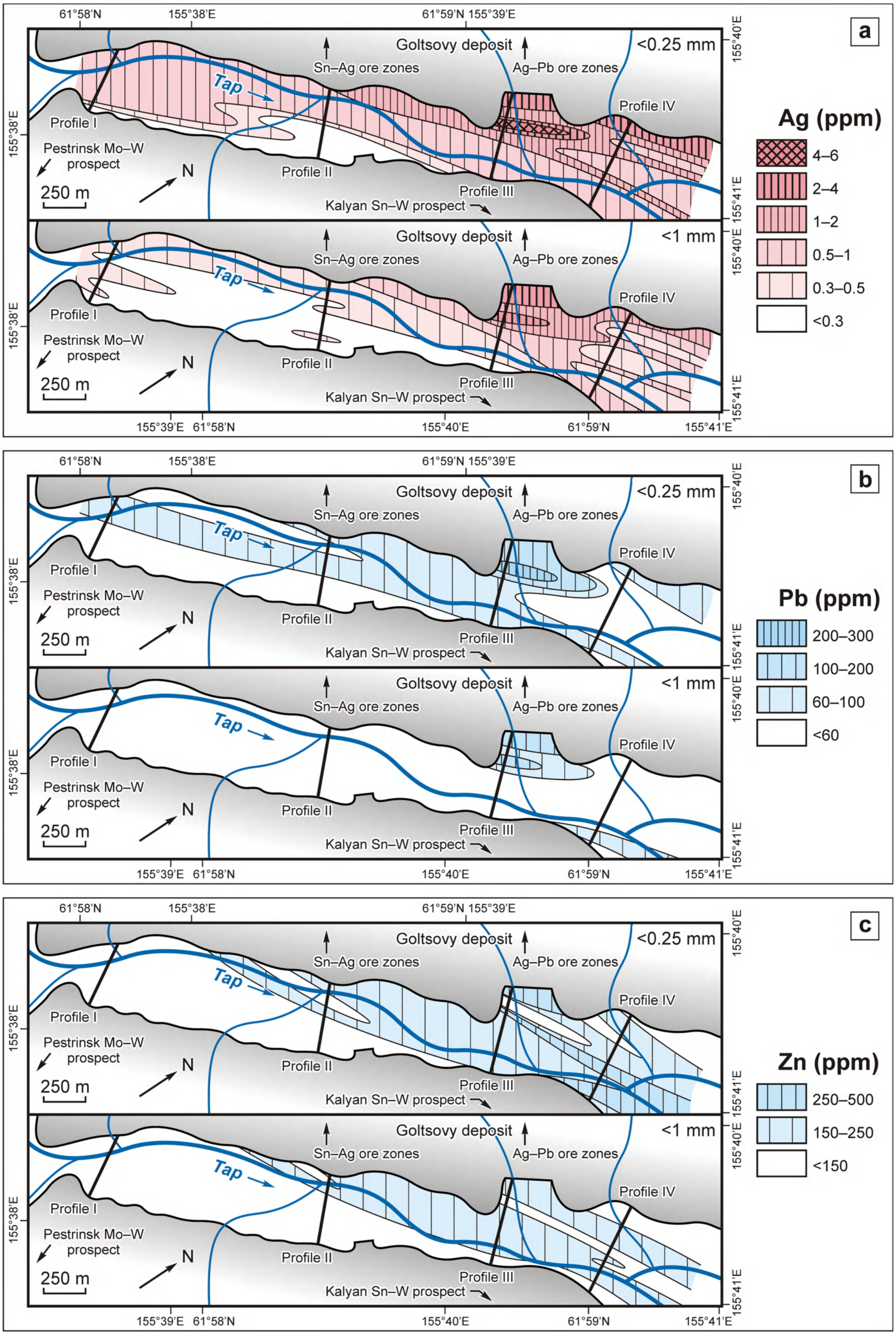

Fig. 6 The Ag (**a**), Pb (**b**) and Zn (**c**) AGFs identified through SSs in Tap River valley (profiles I–IV). Fractions < 0.25 mm and < 1 mm

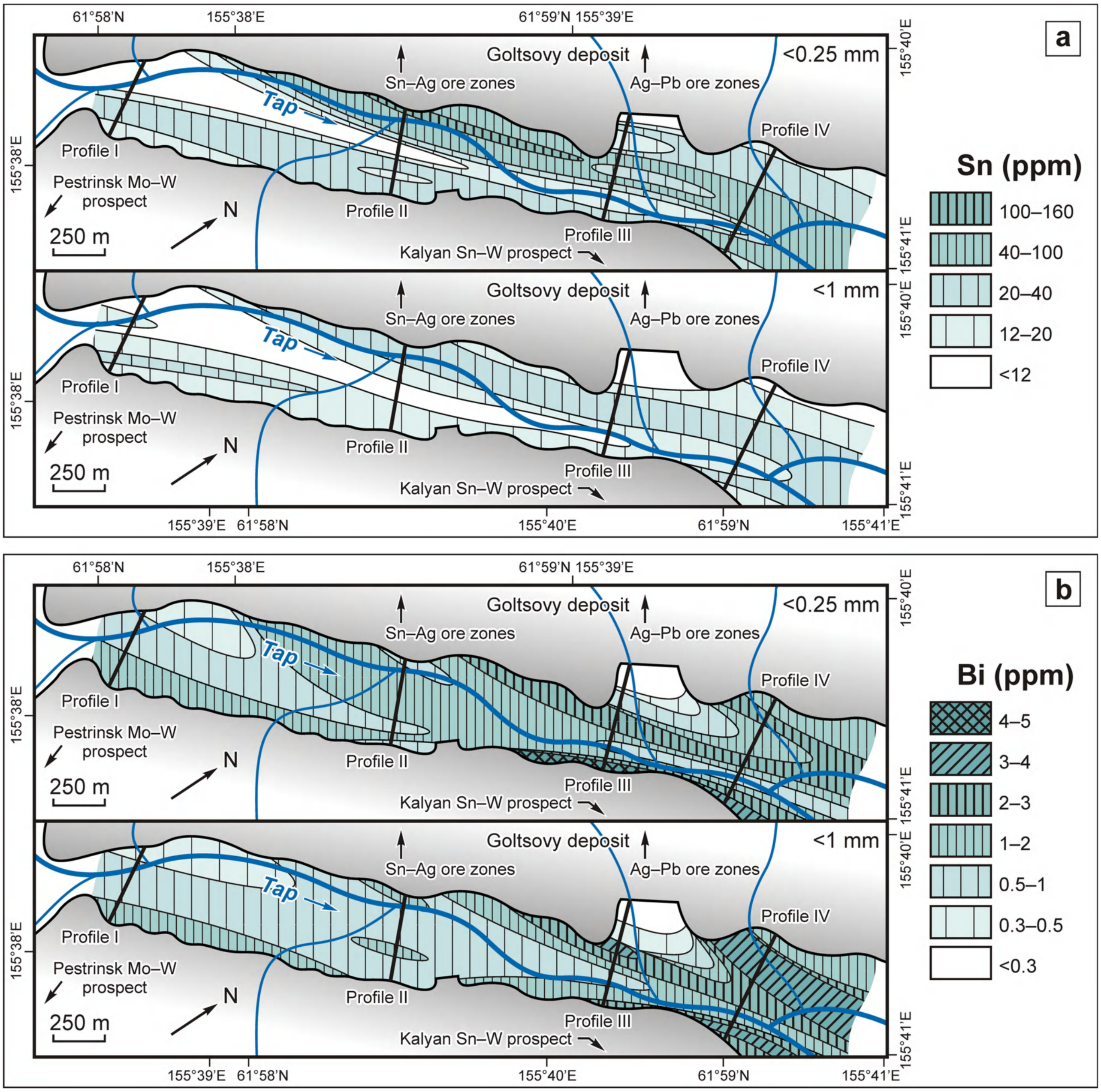

Fig. 7 The Sn (**a**) and Bi (**b**) AGFs identified through SSs in Tap River valley (profiles I–IV). Fractions < 0.25 mm and < 1 mm

identified on the right side of the valley in profile IV, e.g., at the influence place of small water flows draining *Sn–W* mineralization of the Kalyan prospect. The AGFs of Sn with the contents 20–40 ppm (CR = 5–10) were occur in all profiles including the right side of the valley in profiles I and II (Pestrinsk *Mo–W* prospect). The least contrasting fields of Sn (< 20 ppm, CR < 5) were primarily typical of the left side of the valley in profile I, where mineralization is almost not the case, and in profile III (*Ag–Pb* ore zones of the Goltsovy deposit).

The maximum concentrations of Bi (4–5 ppm, CR = 40–50) were detected in profile III on the right side of valley, at place of transported material of *Sn–W* mineralization of the Kalyan prospect (Fig. 7b). The AGFs with lower concentrations (2–4 ppm, CR = 20–40) were identified only in profiles III and IV. These fields extended along the right (Kalyan prospect) and left sides (*Sn–Ag* ore zones and flanks of *Ag–Pb* zones of the Goltsovy deposit) of the valley. The AGFs with concentrations 1–2 ppm (CR = 10–20) were revealed in the other profiles too, including profile II,

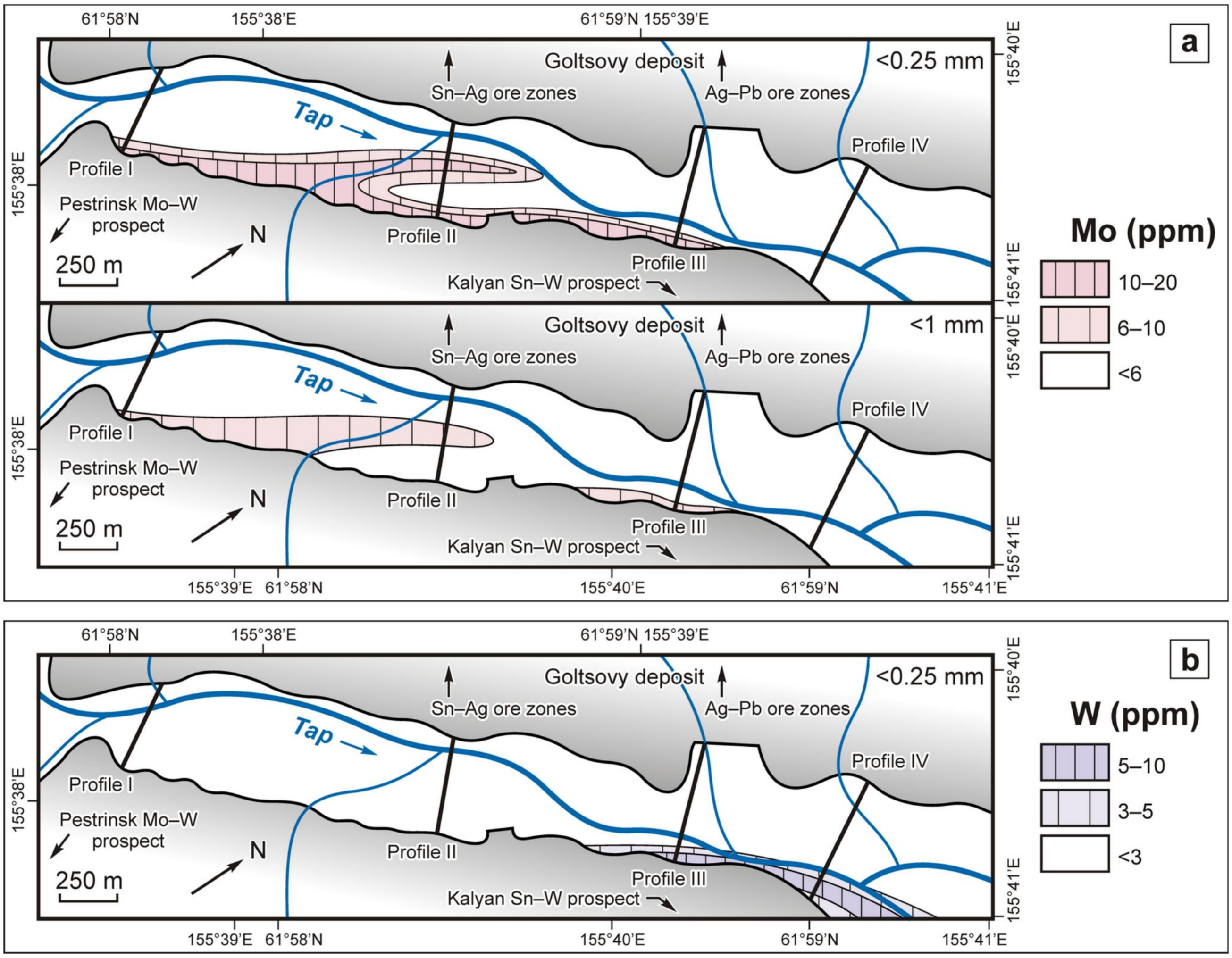

Fig. 8 The Mo (**a**) and W (**b**) AGFs identified through SSs in Tap River valley (profiles I–IV). Fractions < 0.25 mm and < 1 mm

left side (*Sn–Ag* ore of the Goltsovy deposit) and profiles I–II, right side (Pestrinsk *Mo–W* prospect). The Bi AGFs of the lowest contrast (< 0.5 ppm, CR < 5), the same as Sn AGFs, were recognized only on the left side of the valley. They were found in profile I, where ores on the slopes are not present at all, and in profile III, where on the slopes the richest *Ag–Pb* ores of the Goltsovy deposit were prospected.

Molybdenum and *tungsten* in alluvium of the Tap River formed low contrast anomalies, which, moreover, were not detected in all the fractions considered (Fig. 8). The Mo contents in geochemical fields varied within interval from < 6 ppm (CR < 3) to 20 ppm (CR = 10), W contents from < 3 ppm (CR < 3) to 10 ppm (CR = 10). The maximal concentrations of Mo (10–20 ppm, CR = 5–10) were revealed in fraction < 0.25 mm (Fig. 8a). The AGFs of Mo identified in the same fraction of alluvium, covered the largest area. In the common fraction, the Mo contents did not exceed 6–10 ppm at CR = 3–5. The anomalous contents of W (3–10 ppm, CR = 3–10) were available only in the fine fraction (Fig. 8b), whereas in the common fraction, its contents were nearly background (< 3 ppm, CR < 3).

The AGFs of Mo and W were present only on the right side of the Tap River valley, where rare-metal mineralization discovered on the slopes and watershed. The Mo anomalies were most common for the upstream (profiles I–II), where the Pestrinsk *Mo–W* prospect sits on one slope of the Tap River valley. The Mo anomalies were less widespread in profile III (Kalyan *Sn–W* prospect). The AGFs of W were detected only in profiles III–IV at area of the outcropped ore zones of the Kalyan *Sn–W* prospect. The left side of the Tap River valley (*Ag–Pb* and *Sn–Ag* ore zones of the Goltsovy deposit) was typified by nearly background contents of Mo (< 6 ppm, CR < 3) and W (< 3 ppm, CR < 3).

The correlation analysis carried out on all samples (profiles I–IV) and on all alluvium fractions yielded almost no results. Statistically significant relationships can only be established between some elements. This is due to the fact that the same elements can simultaneously serve as

Table 2 Pair correlation coefficients of elements; the Tap River (profiles I–IV), alluvium fraction < 0.25 mm

	Ag	Pb	Zn	Sn	Bi	Mo
Profile I						
Pb	**+ 0.43**					
Zn	**+ 0.42**	+ 0.24				
Sn	− 0.26	**− 0.41**	− 0.16			
Bi	**− 0.30**	− 0.15	− 0.10	**+ 0.47**		
Mo	**− 0.40**	− 0.23	0.00	+ 0.16	**+ 0.61**	
Profile II						
Pb	**+ 0.68**					
Zn	**+ 0.80**	**+ 0.68**				
Sn	**+ 0.45**	**+ 0.45**	**+ 0.49**			
Bi	+ 0.04	**+ 0.42**	**+ 0.31**	− 0.05		
Mo	− 0.28	− 0.18	− 0.14	− 0.12	− 0.01	
Profile III						
Pb	**+ 0.81**					
Zn	**+ 0.41**	**+ 0.54**				
Sn	**− 0.32**	− 0.23	− 0.15			
Bi	**− 0.39**	− 0.15	− 0.10	**+ 0.30**		
Mo	− 0.09	− 0.06	− 0.18	− 0.10	**+ 0.58**	
W	− 0.10	− 0.15	− 0.11	+ 0.01	**+ 0.67**	**+ 0.88**
Profile IV						
Pb	+ 0.18					
Zn	− 0.03	**+ 0.65**				
Sn	− 0.14	**+ 0.50**	**+ 0.65**			
Bi	+ 0.06	+ 0.25	+ 0.23	+ 0.16		
Mo	+ 0.13	**+ 0.33**	+ 0.23	**+ 0.46**	+ 0.25	
W	+ 0.10	**+ 0.49**	**+ 0.44**	**+ 0.35**	**+ 0.31**	**+ 0.37**

The sample size for profiles I, II, III and IV equaled 22, 21, 23 and 24, respectively. Statistically significant correlation coefficients are highlighted in bold. Correlation relationships for W in profiles I and II were not calculated, because its contents in all samples were below the detection limit of the SSA method (< 2 ppm)

indicators for different types of ores. Based on the data obtained, we can assume the presence of only two types of mineralization. *Ag–Pb* ores are most clearly manifested, which is due to its significant predominance over other types of mineralization in the considered site. A strong relationship was established for Ag–Pb (+ 0.75), moderate ones for Pb–Zn (+ 0.45) and Ag–Zn (+ 0.36) (fine fraction). The correlation links are also revealed for rare metal mineralization, although uncertainly. The presence of this mineralization is indicated by the moderate relationships W–Bi (+ 0.51) and Mo–W (+ 0.37) (fine fraction).

More clear relationships between the elements were established by correlation analysis of samples taken along individual profiles. In this case, the fine fraction of alluvium was the most indicative (Table 2).

In profile I, which belongs to area influenced by the Pestrinsk Mo–W prospect, clear relationships have been established between the main indicator elements of this mineralization type. The highest values of pair correlation coefficients were found for Mo–Bi (+ 0.61) and Sn–Bi (+ 0.47). For W, the relationships with other elements could not be established (including profile II), because its contents in all samples taken along profile, I were below the detection limit of the SSA method. Moderate relationships were also established for Ag–Pb (+ 0.43) and Ag–Zn (+ 0.42), which indicates the influence of *Ag–Pb* ores. At the same time, these ores do not correlate at all with rare metal mineralization, as evidenced by the moderate negative relationships for Ag–Mo (− 0.40), Ag–Bi (− 0.30) and Pb–Sn (− 0.41).

In profile II, where *Sn–Ag* mineralization of the Goltsovy deposit (along with *Ag–Pb* ores) is exposed along the left side of the Tap River valley, clear moderate relationships were revealed for Sn–Zn (+ 0.49), Ag–Sn (+ 0.45), Pb–Sn (+ 0.45), Pb–Bi (+ 0.42) and Zn–Bi (+ 0.31). Nevertheless, the main indicator elements of *Ag–Pb* ores have the highest values of correlation coefficients. A strong relationship was established for Ag–Zn (+ 0.80), moderate ones for Ag–Pb (+ 0.68) and Pb–Zn (+ 0.68).

In profile III, the highest values of pair correlation coefficients were typical for the main indicator elements of *Ag–Pb* (Goltsovy deposit) and *Sn–W* (Kalyan prospect) mineralization types. *Ag–Pb* ores are characterized by a strong relationship between Ag and Pb (+0.81), the main elements. Pb–Zn (+0.54) and Ag–Zn (+0.41) had moderate relationships. The presence of *Sn–W* mineralization is indicated by a strong relationship for W–Mo (+0.88) and moderate relationships for W–Bi (+0.67), Mo–Bi (+0.58) and Sn–Bi (+0.30). It should be noted that *Ag–Pb* and *Sn–W* mineralization types do not correlate with each other. This is indicated by the moderate negative relationships Ag–Bi (−0.39) and Ag–Sn (–0.32).

Profile IV is characterized by a wide variety of correlation relationships between elements. Both regular dependencies and non-typical relationships between elements have been established. The moderate relationship for Pb–Zn (+0.65) may indicate the presence of polymetallic mineralization material in this profile. The rare metal mineralization type is indicated by the moderate relationships for Sn–Mo (+0.46), Mo–W (+0.37), Sn–W (+0.35) and Bi–W (+0.31). At the same time, atypically high values of correlation coefficients were revealed for some elements: Sn–Zn (+0.65), Pb–Sn (+0.50), Pb–W (+0.49), W–Zn (+0.44) and Pb–Mo (+0.33). These correlation relationships may indicate the mixing of material of different mineralization (*Ag–Pb* + *Sn–Ag* + *Sn–W*) in profile IV. This is also clearly visible from the AGF distribution of the considered elements in this profile (Figs. 6, 7, 8).

5 Discussion

5.1 Results of sampling SSs of the Maly Ken and Ken Rivers along profiles versus the results of the geochemical survey of SSs at a 1:50 000 scale

When comparing results obtained in the study of AGFs of Au and Ag in profile I with those before received in the geochemical survey of SSs at a 1:50 000 scale over the same area it was feasible to establish the advantages of our proposed method. It is evident that in sampling along profile I the Au and Ag anomalies were most distinctly uncovered. The study of pattern of distribution and concentration levels of Au and Ag in different fractions of alluvium showed that the AGFs identified through fine fraction were maximally contrasting and covering the largest areas. This particularly concerns Au, its contents in this fraction were three times higher than in the common one. The Au and Ag anomalies, the main indicator elements of *Au–Ag* mineralization, were located on the right side of the Maly Ken River valley, closer to the mouth of the Krasin stream draining the *Au–Ag* prospect of the same name (Fig. 4). On this side, they were covering also the largest areas.

In the geochemical survey of SSs at a 1:50 000 scale, with collecting traditional prospecting fraction < 1 mm, the AGFs of Au and Ag in this place of the valley were not detected. The contents of these elements turned to be nearly background: Au < 0.004 ppm at CR < 2 (below detection limit of the AAS method), Ag mainly < 0.02 ppm at CR < 0.2 (below detection limit of the SSA method) (Fig. 9a, Table 3). The reason is that while sampling in the large river valley the alluvium material of a sample collected traditionally was not representative at all. Only one sample was taken within the entire valley width. The share of ore minerals in the analysed common fraction was insignificant as compared to the fine fraction collected along profiles.

Comparing the results obtained in the study of the AGFs of Ag, Pb and Zn, the main indicator elements of *Ag–Pb* mineralization, in profile II in the Ken River valley with the results obtained in the geochemical survey of SSs at a 1:50 000 scale, indicated that the proposed method is advantageous. The anomalies of Ag, Pb and Zn recognized through the fine fraction in profile II showed high contrast and broad distribution. The anomalies extended along the right side of the valley, closer to place of confluence of Gorely stream draining *Ag–Pb* ore zones of the Tidid deposit (Fig. 5). The common fraction was less representative. The contents of Ag, Pb and Zn in it were mainly low. The pattern of the distribution of element contents was uncertain.

At the same time, sampling accomplished in traditional geochemical survey of SSs at a 1:50 000 scale at the site of profile II provided no positive results. The AGFs of Ag, Pb and Zn in the common fraction of alluvium were not identified, and concentrations of these elements did not exceed 0.06 ppm (CR < 0.6), 15 ppm (CR < 0.75) and 100 ppm (CR < 2), respectively (Fig. 9b, Table 4). It is most likely, that samples were taken close to the Maly Ken and Ken riverbeds, showing minimal contents of Ag, Pb and Zn (Fig. 5).

5.2 Results of sampling SSs of the Tap River along profiles versus the results of the geochemical survey of SSs at a 1:50 000 scale

The results of examining alluvium sampled in the Tap River valley by the proposed technique supported its efficiency compared to the geochemical survey of SSs at a 1:50 000 scale. The alluvium fractions (common < 1 mm and fine < 0.25 mm) displayed a distinct pattern of the composition and structure of exogenous AGFs of Ag, Pb, Zn, Sn, Bi, Mo and W, the main indicator elements of *Ag–Pb*, *Sn–Ag*, *Sn–W* and *Mo–W* mineralization, in all four profiles. The fine fraction of alluvium turned to be mostly informative. It showed the highest concentrations of elements, and their pattern of distribution was quite distinct.

The most contrasting AGFs of Ag and Pb extended along the left side of the Tap River valley, its slopes and watershed hosting *Ag–Pb* and *Sn–Ag* ore zones of the Goltsovy deposit (Fig. 6a, b). It is noteworthy that Ag AGFs with contents > 1 ppm (CR > 10) extended from profile II and

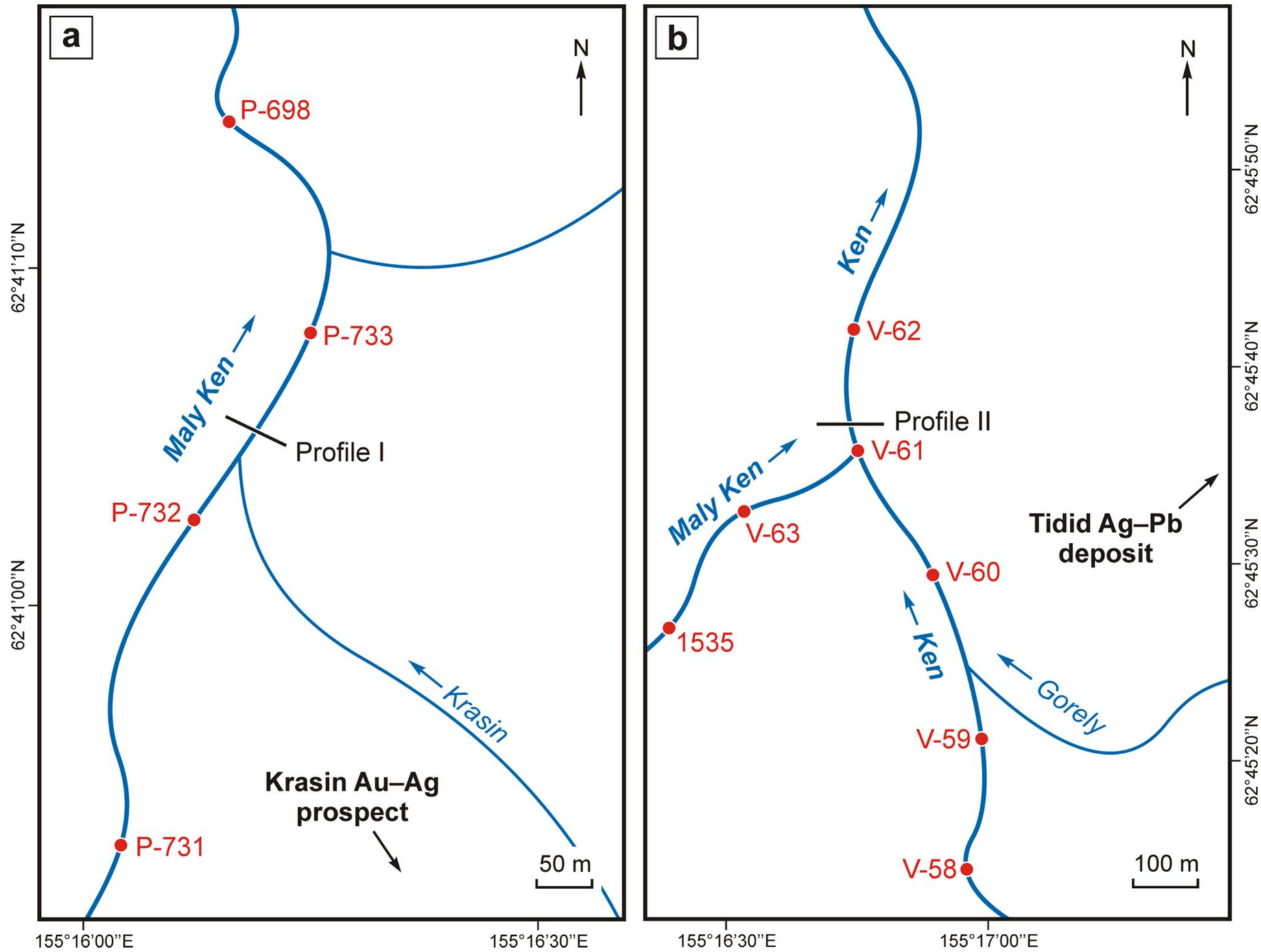

Fig. 9 The locations of alluvium samples on the Maly Ken (**a**, **b**) and Ken (**b**) Rivers in geochemical survey of SSs at a 1:50 000 scale (fragment). Tables 3 and 4 present element contents in samples

Table 3 Contents of Au and Ag in the samples taken in geochemical survey of SSs at a 1:50 000 scale on the Maly Ken River (fraction < 1 mm)

No. sample	Element contents (ppm)	
	Au	Ag
P-731	< 0.004	< 0.02
P-732	< 0.004	< 0.02
P-733	< 0.004	< 0.02
P-698	< 0.004	0.02

For sampling points, see Fig. 9a. Results of the AAS (Au) and SSA (Ag) methods. Here and in Tables 4 and 5: the analyses were carried out at the IGC SB RAS

Table 4 Contents of Ag, Pb and Zn in the samples taken in geochemical survey of SSs at a 1:50 000 scale on the Maly Ken and Ken Rivers (fraction < 1 mm)

No. sample	Element contents (ppm)		
	Ag	Pb	Zn
V-58	0.04	15	100
V-59	0.04	15	80
V-60	0.03	15	100
V-61	0.04	10	60
V-62	0.04	10	100
1535	0.02	10	60
V-63	0.06	15	100

For sampling points, see Fig. 9b. Here and in Table 5: results of the SSA method

downstream through profiles III and IV, i.e. within the influence area of *Sn–Ag* and *Ag–Pb* mineralization, for which Ag is the main typomorphic element. The Pb AGFs with contents > 100 ppm (CR > 5) were recognized only in profile III, in the influence area of *Ag–Pb* ores, for which this element is the main one. Further, upstream of the Tap River from profile II to profile I on the left side of the valley, where

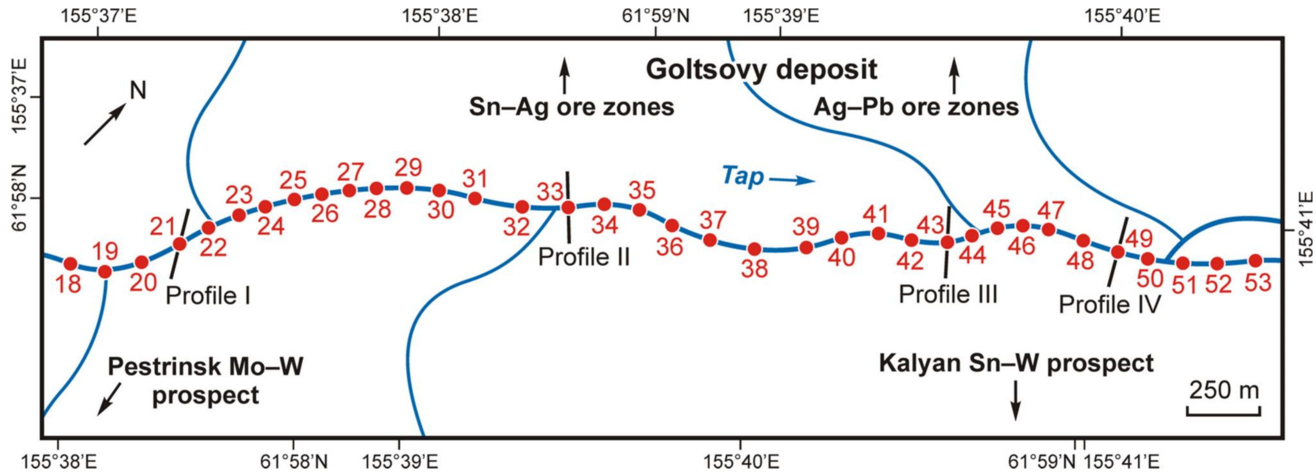

Fig. 10 The locations of alluvium samples on the Tap River in geochemical survey of SSs at a 1:50 000 scale (fragment). Table 5 presents element contents in samples

Table 5 Contents of Ag, Pb, Zn, Sn, Bi, Mo and W in the samples taken in geochemical survey of SSs at a 1:50 000 scale on the Tap River (fraction < 1 mm)

No. sample	Element contents (ppm)							No. sample	Element contents (ppm)						
	Ag	Pb	Zn	Sn	Bi	Mo	W		Ag	Pb	Zn	Sn	Bi	Mo	W
18	1.5	50	100	15	1	5	< 2	36	3	50	300	15	1.5	6	< 2
19	2	50	200	10	0.8	5	< 2	37	3	50	300	20	1.5	5	< 2
20	2	50	200	10	0.8	5	< 2	38	3	50	200	20	2	5	< 2
21	2	50	200	10	0.8	5	< 2	39	3	50	200	20	2	5	< 2
22	2	50	300	10	0.8	5	< 2	40	3	50	300	20	2	6	< 2
23	2	50	150	10	1	5	< 2	41	3	50	300	20	2	6	< 2
24	1.5	50	200	10	0.8	5	< 2	42	3	50	400	20	2	5	< 2
25	3	50	200	10	1	5	< 2	43	3	50	300	20	1.5	5	< 2
26	2	50	200	15	1	5	< 2	44	1	50	300	15	2	5	< 2
27	2	50	300	15	1.5	5	< 2	45	2	50	300	20	2	5	< 2
28	3	50	300	15	1	5	< 2	46	2	50	300	20	2	5	< 2
29	3	50	200	20	1.5	5	< 2	47	2	50	200	30	1.5	5	< 2
30	3	50	200	15	1.5	6	< 2	48	2	50	200	20	1.5	5	< 2
31	3	50	200	15	1	6	< 2	49	2	50	200	20	2	5	< 2
32	3	50	200	15	1	6	< 2	50	2	50	200	20	3	5	< 2
33	2	50	200	30	1.5	6	< 2	51	2	50	300	30	1.5	5	< 2
34	2	50	200	15	1	6	< 2	52	2	50	300	30	1.5	5	< 2
35	3	50	200	15	1.5	6	< 2	53	2	50	300	30	2	5	< 2

For sampling points, see Fig. 10

Ag–Pb and *Sn–Ag* mineralization is not available, as well as towards the right side of the valley involving the rare-metal prospects, the Ag and Pb concentrations noticeably decreased up to nearly background.

A clear pattern was also observed for the most contrasting AGFs of Zn. The Zn AGFs were identified on the left side of the valley (profile III), within the influence area of *Ag–Pb* mineralization of the Goltsovy deposit, for which Zn is typomorphic, and on the right side (profile IV), where the ore bodies of the Kalyan *Sn–W* prospect crop out, for which this element is also common (Fig. 6c). Less contrasting fields of Zn were found on the left side of the valley in profile II, with *Sn–Ag* ore zones of the Goltsovy deposit. Zn is the secondary indicator elements for this type of mineralization.

Comparison with the alluvium samples collected at the segment of the Tap River covered in survey of SSs at a 1:50 000 scale (fraction < 1 mm) showed that Ag concentrations in them did not exceed 3 ppm (CR < 30), Zn mainly 300 ppm (CR < 6) (Fig. 10, Table 5). Through the entire site, Pb contents amounted to 50 ppm (CR = 2.5) (Fig. 10,

Table 5). The pattern of distribution of these elements was not revealed. It was impossible to locate from which side of the valley loose sediments with such contents were transported. Attention should be paid to the high contents of Ag found in traditional geochemical survey. In most samples, they were 2–3 ppm (Table 5). In this case, the explanation is simple. In the Tap River upstream, the samples were taken at the foot of the left flat slope hosting unprofitable zones of *Sn–Ag* mineralization. The ore material, even if not rich in Ag content, arrives directly to the loose sediments of the river. Downstream along the left side of the Tap River valley does not show any outcrop of mineralization. The richest in silver content *Ag–Pb* ore zones of the Goltsovy deposit are located on the watershed remotely from the Tap River. The loose material is transported to the Tap River by two water streams draining these ore zones. While the SSs are being formed, the supplied material is impoverished, so the Ag concentrations decrease. As a result, there is no differentiation in the Ag content in all samples collected within the valley in the survey of SSs at a 1:50 000 scale. The Ag contents are similar and do not depend on the scale and profitable value of available mineralization.

The distinct pattern was also observed in the composition and structure of exogenous AGFs of Sn and Bi. The Sn anomalies with contents > 100 ppm (CR > 25) were detected only on the left side of the Tap River valley. They were identified in profile II, at the influence site of *Sn–Ag* ore zones of the Goltsovy deposit (Fig. 7a). The less contrasting fields of Sn with concentrations 40–100 ppm (CR = 10–25) had a wider distribution. They were recognized in profiles II, III and IV and were linked with *Sn–Ag* mineralization. The Sn anomalies were well established on the right side of the valley (profile IV), its slopes involving the Kalyan *Sn–W* prospect. Whereas the maximally anomalous fields of Bi with contents > 4 ppm (CR > 40) extended only along the right side of the river valley. They were identified in profile III and show relationship with Kalyan prospect (Fig. 7b). The Bi AGFs with contents 2–4 ppm (CR = 20–40) were revealed on the left side of the valley from profile II downstream through profiles III and IV. The effect of *Sn–Ag* ore zones of the Goltsovy deposit and the flanks of its *Ag–Pb* zones (profile IV) was obvious there. To summarize, in the direction from the left side of the valley to the right one, the following pattern is obvious: the Sn content in AGFs decreased, and that of Bi content increased. This pattern is explained by the outcrop on the left side of *Sn–Ag* ore zones of the Goltsovy deposit, for which a higher Sn content is common, while on the right side it is the Kalyan *Sn–W* prospect, its ore zones having high Bi contents. Presence of the least contrasting fields of Sn and Bi in the other parts of the valley is explained by the fact, that ores are extremely poor there, or there is unprofitable sulphide mineralization typified by low contents of Sn and Bi.

In the alluvium samples collected in survey at a 1:50 000 scale on the explored segment of the Tap River valley, the Sn contents were < 30 ppm (CR < 7.5) and Bi mainly 2 ppm (CR < 20) (Fig. 10, Table 5). The more detailed analysis of distribution of these elements along the flow provides some specifics. In the samples, collected in the river upstream the Sn contents were 10–20 ppm (CR = 2.5–5), and downstream they varied from 20 to 30 ppm (CR = 5–7.5). The Bi contents in the upstream were 0.8–1.5 ppm (CR = 8–15), and downstream they were 2–3 ppm (CR = 20–30). The tendency is observed in increasing the Sn and Bi contents downstream, that is linked with the supply in the alluvium of ore material of *Sn–Ag* (flanks of the Goltsovy deposit) and *Sn–W* (Kalyan prospect) mineralization. However, it was impossible to locate the side of the valley from which loose sediments were transported, as in the case with Ag, Pb and Zn, although the pattern of element distribution was recognized in survey at a 1:50 000 scale.

For Mo and W, the main indicator elements of *Sn–W* and *Mo–W* mineralization, even if they had low contents in SSs of the Tap River, there was a clear pattern in the distribution (Fig. 8). The Mo and W anomalies were present only in the right side of the valley, where its slopes expose the rare-metal mineralization. To note, the exogenous AGFs of Mo identified upstream in profiles I–III mainly occurred at the sites of *Mo–W* mineralization (Pestrinsk prospect). The W anomalies located downstream in profiles III and IV commonly occurred at the sites of exposed *Sn–W* ore zones (Kalyan prospect). This specific is explained by the evidence that in *Mo–W* ores the Mo contents dominate over W, and in *Sn–W* ores this element shows low grades versus W. Yet, the left side of the Tap River valley was characterized by nearly background contents of these elements, as on the slopes and watershed the *Ag–Pb* and *Sn–Ag* mineralization (Goltsovy deposit) is present, in which Mo and W are not typical.

Very low concentrations of Mo (< 6 ppm, CR < 3) close to the background were identified in the traditional geochemical survey of SSs at a 1:50 000 scale in alluvium of the Tap River, when compared to the level of concentration of this element in profiles (Fig. 10, Table 5). Any pattern of this element distribution was not determined. The W anomalies in the considered river section were not found as well. The contents of this element were below detection limit of the SSA method (< 2 ppm, CR < 2) (Fig. 10, Table 5).

5.3 Efficiency of sampling SSs of large river valleys along profiles

The detailed investigations point out that the choice of the technique for sampling loose sediments of large river valleys is truly critical. The traditional approaches of sampling accepted in geochemical survey of SSs, under cryolithogenesis conditions of the arctic and subarctic landscapes showed low efficiency. To acquire the reliable information, the number of samples collected along the riverbed is insufficient. It is often the case that in sampling procedure it is impossible to establish the boundaries between the terraces above the flood land and flood land itself, as well as the difference between the loose material (alluvium) and colluvial sediments occurring near the slope foot.

In searching for diverse mineralization (e.g., *Au–Ag*, *Ag–Pb*, *Sn–Ag*, *Mo–W* and *Sn–W*), for a more reliable recognition of the AGFs of ore elements trough loose sediments of large river valleys of IV order, in geochemical survey of SSs under the cryolithogenesis conditions, the most effective is sampling along the profiles located across these valleys. The profiles should be placed below the mouth of lateral tributaries of the river.

Specific features of composition and structure of the exogenous AGFs discovered in the profiles oriented across the river valleys, most completely reflect the ones of eroded and drained deposits and prospects. The contents of indicator elements of mineralization, although it depends on many factors (relief, branching of drainage system, scales and type of mineralization, morphology of ore bodies and their position in space, predominance of physical weathering over chemical processes, specifics of element behaviour in supergene environments and their binding forms), are in general regularly distributed.

The most contrasting exogenous AGFs tend to that side of the valley, where its slope exposes ores. The qualitative-and-quantitative composition of identified anomalies directly depends on the composition of this ores.

Example 1. On the right side of the Maly Ken River valley (profile I), closer to the place of the Krasin stream confluence draining the *Au–Ag* prospect of the same name, there were clearly established AGFs of Au and Ag, the main ore-forming elements. Despite the relatively low values of the correlation coefficients, it can be argued that there is a relationship between these elements, although weak. Poor correlation may be explained by the fact that a significant part of the Ag anomalies is associated with a variety of silver minerals, which at the Krasin Au–Ag prospect is more abundant than gold minerals. At the same time, gold is represented only by electrum and kustelite. As a result, Ag anomalies are almost not accompanied by Au anomalies.

Example 2. On the right side of the Ken River valley (profile II), below the confluence of the Gorely stream draining the *Ag–Pb* ore zones of the Tidid deposit there were AGFs of Ag, Pb and Zn, the main indicator elements of the *Ag–Pb* mineralization. Correlation analysis also confirmed clear relationships between Ag, Pb and Zn.

Example 3. The maximally anomalous exogenous geochemical fields of Ag and Pb, were distinctly identified at the place where the slope (left side of the Tap River valley, profile III) of *Ag–Pb* ore zones of the Goltsovy deposit emerges on the surface. The less contrasting AGFs were typical for Sn, Zn Bi, the secondary ore elements. The same pattern of element distribution is characteristic for *Ag–Pb* ores of this deposit. The *Sn–Ag* ore zones on the flanks of the Goltsovy deposit (left side of the Tap River valley, profile II) were marked by maximally anomalous exogenous fields of Sn and Ag. The AGFs of less high contrast were identified for Bi, Pb and Zn, the secondary ore elements. The same features of element distribution are typical for *Sn–Ag* zones of the Goltsovy deposit. The anomalies of Sn, Bi, Mo and W, the main indicator elements of rare-metal type of ores, tend to the right side of the Tap River valley, its slopes host mineralization of the Pestrinsk (*Mo–W*) and Kalyan (*Sn–W*) prospects. The AGFs of Ag, Pb and Zn showed minor concentrations. These elements are secondary and are found intermittently even in the rare-metal ores itself. All established patterns are also clearly reflected in the pair correlation coefficients. SSs associated with *Ag–Pb* and *Sn–Ag* ore zones of the Goltsovy deposit are characterized by significant relationships between Ag, Pb and Zn, and between Ag, Zn, Pb, Sn and Bi, respectively. For SSs of rare metal mineralization, W, Mo, Bi and Sn have distinct relationships.

This was the fine fraction (<0.25 mm) of alluvium that was found to be most informative, as it had the highest contents of the main indicator elements (Au, Ag, Pb, Zn, Sn, Bi, Mo and W) of diverse mineralization and distinctly displayed the specific features in their distribution. Sampling this fraction in the large river valleys present not difficulties. Loose sediments are well formed, and the sandy silt material is abundant.

The enrichment of the fine fraction of alluvium with ore elements is typical for many deposits of Au, Ag and base metals (e.g., Chork and Cruikshank 1984; Day and Fletcher 1989; Melo and Fletcher 1999; Ali et al. 2015; Yilmaz et al. 2015, 2017, 2019, 2020, 2022; Simmonds et al. 2016). The Au and Ag deposits that we studied (Balygychan–Sugoy trough, North–East of Russia) are not exceptions (Kravtsova and Pavlova 2010; Kravtsova et al. 2010a, b, 2016; Makshakov and Kravtsova 2018, 2021; Makshakov et al. 2019). Most interesting results were obtained in studying loose alluvial sediments of streams draining the *Au–Ag* ores of the Dukat deposit. It is noteworthy, this deposit is located 11 km south of the Krasin *Au–Ag* prospect reported in this paper. Examination of exogenous AGFs at the Dukat deposit also confirmed the efficiency of using fine fraction for their discovery and assessment. It was found that the largest amount of ore minerals occurs in fraction <0.25 mm of alluvial sediments. The highest contents of indicator elements of *Au–Ag* mineralization was common for this particular fine fraction of alluvium.

Some publications (Kravtsova and Pavlova 2010; Kravtsova et al. 2010a, b, 2016; Makshakov and Kravtsova 2018; Makshakov et al. 2019) report not only the results of investigations of the composition and structure of geochemical fields identified through SSs. Significant pioneering information was also received on the binding forms of indicator elements on the *Au–Ag* mineralization in the secondary (supergene) environments. The investigations of alluvial sediments in the water streams draining *Au–Ag* ore zones of the Dukat deposit, showed that native gold proper is found in the loose sediments mainly in the upstream. While the ore material is being transported over the water flow, it becomes impoverished. On the background of Au concentration decrease in the downstream clearly displays the tendency of increasing the number of finely dispersed and "invisible" Au associated with sulphide minerals, mainly pyrite.

In volcanogenic *Au–Ag* deposits of the North–East of Russia pyrite is the most widespread sulphide mineral and main mineral-concentrator of Au in ores and SSs (Kravtsova and Solomonova 1985; Kravtsova and Andrulaytis 1989; Kravtsova 2010; Kravtsova and Pavlova 2010; Kravtsova et al. 2010b, 2015, 2016). Pyrite concentrates gold both at *Au–Ag* deposits, as well as the deposits of the other gold ore formations (e.g., Wells and Mullens 1973; Cambel et al. 1980; Cook and Chryssoulis 1990; Fleet et al. 1993; Simon et al. 1999; Pals et al. 2003; Palenik et al. 2004; Morishita et al. 2008, 2018; Large et al. 2009; Thomas et al. 2011; Deditius et al. 2014; Tauson et al. 2014; Zhang et al. 2018; Gao et al. 2019; Large and Maslennikov 2020; Liu et al. 2020; Ishida et al. 2022; Kravtsova et al. 2022; Zhang et al. 2022; Ehrig et al. 2023; Lin et al. 2023).

The Krasin *Au–Ag* prospect is not an exception. We suspect that pyrite is also the main mineral-concentrator of Au both in ores of this prospect and in the supergene environments (alluvium). In loose sediments of the Krasin stream draining the *Au–Ag* zones, the amount of pyrite in fine fraction reaches 10%–15%. Based on previous data obtained at the Dukat deposit (Kravtsova and Pavlova 2010; Kravtsova et al. 2010b, 2016), we assume that the finely dispersed and "invisible" impurity forms also represent the main binding forms of Au in pyrites of loose sediments of the Krasin stream. In fact, pyrite is unsteady under supergene environments. When in the water flow, it is easily oxidized and destroyed. One part of impurity Au is easily adsorbed by iron hydroxides if pyrite is broken, while the other one is partly retained in its corroded and destroyed grains (Kravtsova and Pavlova 2010; Kravtsova et al. 2010b, 2016). Therefore, the fine fraction bearing the largest amount of this material is particularly rich in Au.

6 Conclusions

The studies described herein provide the evidence that the right choice of the technique is particularly essential for sampling alluvium in the large river valleys. The sampling traditionally undertaken along the riverbeds or over two parallel routes passing on both sides of the valley closely to the slopes (generally accepted in geochemical survey of SSs) seems to be ineffective. To reliably recognize the AGFs of ore elements in geochemical surveys, it makes sense to sample SSs in the large river valleys of IV order along the profiles oriented across the valleys.

The geochemical fields identified by such sampling clear reflect the composition and structure of eroded and drained ore zones. Mostly contrasting AGFs are located on that side of the valley where the slopes crop out the mineralization; qualitative-and-quantitative composition of identified anomalies is basically defined by the composition of this mineralization.

It was found out, that fine fraction (<0.25 mm) of alluvium yields the most complete and accurate pattern of the nature, specific features of distribution and concentration levels of ore elements in loose sediments of large water flows. It steadily has maximum contents of indicator elements of mineralization. The described pattern of their distribution within SSs is specified quite distinctly. Sampling of fine fraction (sandy silt material) in the river valleys of the IV order is easy as this material is available in substantial amounts.

The technique developed for sampling loose alluvial sediments in the large river valleys to recognize the AGFs appears to be simple. It can be used at all stages of geochemical survey, let it be the prognostic evaluation of mineralization on poorly studied areas, or detailed investigations at the sites where a considerable amount of prospecting and assessment works have been implemented. The proposed method is promising in terms of a broad use not only on the territories of the North–East of Russia. It might also be employed effectively in the other regions with similar landscape conditions, primarily where stream sediments are formed under conditions of cryolithogenesis.

Acknowledgements The authors are sincerely grateful to all the geological services of the Dukat Geological Survey (Magadan, Russia) for proper assistance in conducting field works and providing information materials as reports, maps and schemes.

Funding This study was performed within the framework of the State Assignment Projects No. 0284–2021-0002. We used the scientific equipment of the "Isotope-Geochemical Research" Centre for Common Use of IGC SB RAS, Irkutsk, Russia.

Declarations

Conflict of interest The authors declare that they have no conflict of interest.

References

Ali L, Williamson BJ, Moon CJ, Shah MT, Khattak SA (2015) Distribution of gold in different size fractions of stream sediments as a guide to bedrock gold mineralisation along the Shyok Suture Zone and adjacent areas of the Kohistan Island Arc, Pakistan. Arab J Geosci. 8:2227–2235 https://doi.org/10.1007/s12517-014-1306-1

Ayari J, Barbieri M, Barhoumi A, Belkhiria W, Braham A, Dhaha F, Charef A (2022) A regional-scale geochemical survey of stream sediment samples in Nappe zone, northern Tunisia: implications for mineral exploration. J Geochem Explor. 235:106956 https://doi.org/10.1016/j.gexplo.2022.106956

Azmi H, Moarefvand P, Maghsoudi A (2021) Gold anomaly ranking based on stream sediment geochemistry in the Fariman-Kashmar axis, NE Iran. Acta Geochim. 40(2):135–149 https://doi.org/10.1007/s11631-020-00420-8

Belyi VF (2008) Problems of geological and isotopic age of the Okhotsk-Chukotsk Volcanogenic Belt (OCVB). Stratigr Geol Correl. 16:639–649 https://doi.org/10.1134/S086959380806004X

Bogolyubov AN, Sochevanov NN (1959) Small-scale metallometric searches for polymetals on halos and stream sediments. Razved Ohr Nedr. 10:9–12 (**in Russian**)

Boyle RW, Koehler GF, Moxham RL, Palmer HC (1958) Heavy metal, Zn, Cu, Pb, content of water and sediments in streams, rivers and lakes, southwestern Nova Scotia. Geol Surv Can https://doi.org/10.4095/101217

Bradshaw PMD, Clews DR, Walker JL (1972) Exploration geochemistry. Barringer Research Ltd, Rexdale

Cambel B, Stresko V, Sherencakova O (1980) The contents of gold in pyrites of various genesis. Geol Zb Geol Carp. 31:139–159

Chen X, Zheng YY, Xu RK, Wang HM, Jiang XJ, Yan HZ, Cai PJ, Guo XZ (2016) Application of classical statistics and multifractals to delineate Au mineralization-related geochemical anomalies from stream sediment data: a case study in Xinghai-Zeku, Qinghai, China. Geochem Explor Environ Anal. 16:253–264 https://doi.org/10.1144/geochem2016-424

Chork CY, Cruikshank BI (1984) Statistical map analysis of regional stream-sediment data from Australia. J Geochem Explor. 21:405–419 https://doi.org/10.1016/0375-6742(84)90064-5

Cook NJ, Chryssoulis SL (1990) Concentrations of “invisible gold” in the common sulfides. Can Miner. 28:1–16

Dahlberg EC (1968) Application of a selective simulation and sampling technique to the interpretation of stream-sediment copper anomalies near South mountain, Pennsylvania. Econ Geol. 63:409–417 https://doi.org/10.2113/gsecongeo.63.4.409

Day SJ, Fletcher WK (1989) Effects of valley and local channel morphology on the distribution of gold in stream sediments from Harris Creek, British Columbia, Canada. J Geochem Explor. 32:1–16 https://doi.org/10.1016/0375-6742(89)90040-X

Deditius AP, Reich M, Kesler SE, Utsunomiya S, Chryssoulis SL, Walshe J, Ewing RC (2014) The coupled geochemistry of Au and As in pyrite from hydrothermal ore deposits. Geochim Cosmochim Acta. 140:644–670 https://doi.org/10.1016/j.gca.2014.05.045

Degrys A (1961) Copper, lead and zinc in rivers draining Chilean Andes. Econ Geol. 56:1456–1464 https://doi.org/10.2113/gsecongeo.56.8.1456

Ehrig K, Ciobanu CL, Verdugo-Ihl MR, Dmitrijeva M, Cook NJ, Slattery AD (2023) Lifting the cloak of invisibility: gold in pyrite from the Olympic Dam Cu-U-Au-Ag deposit, South Australia. Am Miner. 108:259–276 https://doi.org/10.2138/am-2022-8395

Filosofov VP (1975) Fundamentals of the morphometric method of prospecting for tectonic structures. Saratov University, Saratov (**in Russian**)

Fleet ME, Chryssoulis SL, MacLean PJ, Davidson R, Weisener CG (1993) Arsenian pyrite from gold deposits: Au and As distribution investigated by SIMS and EMP, and color staining and surface oxidation by XPS and LIMS. Can Miner. 31:1–17

Gao FP, Du YS, Pang ZS, Du YL, Xin FP, Xie JS (2019) LA-ICP-MS trace-element analysis of pyrite from the Huanxiangwa gold deposit, Xiong’ershan District, China: implications for ore genesis. Minerals. 9:157 https://doi.org/10.3390/min9030157

Goncharov VI, Alshevsky AV, Vortsepnev VV (1984) Geology and minerals of north-east Asia. Nauka, Vladivostok (**in Russian**)

Grigoryan SV, Solovov AP, Kuzin MF (1983) Instruction on geochemical prospecting for ore deposits. Nedra, Moscow (**in Russian**)

Hawkes HE, Bloom H (1956) Heavy metals in stream sediment used as exploration guides. Min Eng. 8:1121–1126

Hawkes HE, Webb JS (1962) Geochemistry in mineral exploration. Harper & Row, New York

Horton RE (1945) Erosional development of streams and their drainage basins; hydrophysical approach to quantitative morphology. Geol Soc Am Bull. 56:275–370 https://doi.org/10.1130/0016-7606(1945)56[275:EDOSAT]2.0.CO;2

Ishida M, Romero R, Leisen M, Yasukawa K, Nakamura K, Barra F, Reich M, Ya K (2022) Auriferous pyrite formed by episodic fluid inputs in the Akeshi and Kasuga high-sulfidation deposits, Southern Kyushu, Japan. Miner Depos 57:129–145 https://doi.org/10.1007/s00126-021-01053-4

Kiryukhin VA, Shvets VM (2010) Groundwater runoff—key problem of regional hydrogeology. Proc High Educ Establ Geol Explor. 5:42–47 (**in Russian**)

Kitaev NA (1990) Multidimensional analysis of geochemical fields. Nauka, Novosibirsk (**in Russian**)

Konstantinov MM, Rosenblum IS, Strujkov SF (1993) Types of epithermal silver deposits, northeastern Russia. Econ Geol. 88:1797–1809 https://doi.org/10.2113/gsecongeo.88.7.1797

Konstantinov MM, Natalenko VE, Kalinin AI, Strujkov SF (1998) Dukat gold-silver deposit. Nedra, Moscow (**in Russian**)

Konstantinov MM, Kostin AV, Sidorov AA (2003) The geology of silver ore deposits. SUE NPPC “Sakhapolygraphizdat,” Yakutsk (**in Russian**)

Kravtsova RG (2010) Geochemistry and forming conditions of gold-silver ore-forming systems, Northern Pre Okhotsk Region. Academic Publishing House “Geo,” Novosibirsk (**in Russian**)

Kravtsova RG, Andrulaytis LD (1989) Forms of occurrence of gold, silver and mercury and their distribution patterns in ores and endogenous haloes of gold-silver deposits. Trans (dokl) USSR Acad Sci Earth Sci Sect. 307:180–183

Kravtsova RG, Solomonova LA (1985) Gold in pyrite from ores and metasomatites of the gold-silver deposits in the North Okhot’ye volcanogenic fields. Geochem Int. 22:9–14

Kravtsova RG, Zakharov MN (1996) Geochemical concentration fields of Dukat gold–silver bearing ore magmatic system (North–East Russia). Geol Geofiz. 37:28–38 (**in Russian**)

Kravtsova RG, Zakharov MN, Ivanov OP (1996) Combined geochemical investigations of the Pestrinsk silver-bearing field (Northeast Russia). Geol Ore Depos. 38:378–389

Kravtsova RG, Zakharov MN, Shatkov NG (1998) Mineralogical and geochemical features of host rocks of the Gol’tsovoe silver-base metal deposit (Northeastern Russia). Geol Ore Depos. 40:197–210

Kravtsova RG, Borovikov AA, Borisenko AS, Prokof’ev VY (2003) Formation conditions of gold–silver deposits in the northern Okhotsk region, Russia. Geol Ore Depos. 45:395–415

Kravtsova RG, Pavlova LA, Rogozina YuI (2010a) Modes of Ag occurrence in the loose deposits of dispersal trains at Au–Ag mineral deposits. Geochem Int. 48:731–736 https://doi.org/10.1134/S0016702910070104

Kravtsova RG, Pavlova LA, Rogozina YuI, Makshakov AS (2010b) First data on forms of gold occurrence in lithochemical sedimental streams of the gold–silver Dukat deposit (Northeastern Russia). Dokl Earth Sci. 434:1184–1191 https://doi.org/10.1134/S1028334X10090096

Kravtsova RG, Makshakov AS, Pavlova LA (2015) Mineral and geochemical compositions, regularities of distribution, and specific formation of ore mineralization of the Rogovik gold-silver deposit (northeastern Russia). Russ Geol Geophys. 56:1367–1383 https://doi.org/10.1016/j.rgg.2015.09.001

Kravtsova RG, Tarasova YI, Makshakov AS, Pavlova LA (2016) Distribution and modes of occurrence of Au, Ag, and associated elements in the sediment streams of Au–Ag zones at the Dukat deposit (Northeastern Russia). Russ Geol Geophys. 57:529–548 https://doi.org/10.1016/j.rgg.2015.03.017

Kravtsova RG, Makshakov AS, Tauson VL, Belozerova OYu, Tatarinov VV (2022) Speciation features of gold in ores and minerals of the Natalkinskoe deposit (North-East Russia). Geodyn Tectonophys. 13:0595. https://doi.org/10.5800/GT-2022-13-2s-0595. (**in Russian with English abstract**)

Kravtsova R, Pavlova L (2010) Determination of modes and structure of gold and silver occurrence in Hypergene deposits by electron probe microanalysis method (exemplified by loose sediments of water currents of the Dukat deposit). In: Proceeding National of the Academy of Sciences Bulgaria. Materials of 10th International Multidisciplinary Scientific Geoconference, vol. 1: Geology. SGEM, Albena, pp 1–8

Kuznetsov VM, Livach AE (2005) Construction and metallogenic zoning of the Balygychan-Sugoy trough. In: Goncharov VI, Kuznetsov VM (eds) Problems of metallogeny of ore regions in North-East of Russia: proceedings. NEISRI FEB RAS, Magadan, pp 156–177 (**in Russian**)

Kvashnevskaya NV (1957) Prospecting for ore deposits on stream sediments. Geochemical prospecting for ore deposits in the USSR. Gosgeoltekhizdat, Moscow, pp 146–157 (**in Russian**)

Large RR, Maslennikov VV (2020) Invisible gold paragenesis and geochemistry in pyrite from orogenic and sediment-hosted gold deposits. Minerals. 10:339 https://doi.org/10.3390/min10040339

Large RR, Danyushevsky L, Hollit C, Maslennikov V, Meffre S, Gilbert S, Bull S, Scott R, Emsbo P, Thomas H, Singh B, Foster J (2009) Gold and trace element zonation in pyrite using a laser imaging technique: implications for the timing of gold in orogenic and Carlin-style sediment-hosted deposits. Econ Geol. 104:635–668 https://doi.org/10.2113/gsecongeo.104.5.635

Lin X, Hu YQ, Meng GG, Zhang MM (2020) Geochemical patterns of Cu, Au, Pb and Zn in stream sediments from Tongling of East China: compositional and geostatistical insights. J Geochem Explor. 210:106457 https://doi.org/10.1016/j.gexplo.2019.106457

Lin CG, Yao XF, Mao JW, Yan TJ, Cheng ZZ, Mi KF, Jia HX, Lin LJ (2023) Source of ore-forming fluid and material in the Baiyun gold deposit, Liaoning Province, NE China: constraints from H-O-S-Pb isotopes and in-situ analyses of Au-bearing pyrites. J Earth Sci. 34:1–19 https://doi.org/10.1007/s12583-021-1420-4

Lipp AG, de Caritat P, Roberts GG (2023) Geochemical mapping by unmixing alluvial sediments: an example from northern Australia. J Geochem Explor. 248:107174 https://doi.org/10.1016/j.gexplo.2023.107174

Liu Y, Cheng QM, Xia QL, Wang XQ (2014) Multivariate analysis of stream sediment data from Nanling metallogenic belt, South China. Geochem Explor Environ Anal. 14:331–340 https://doi.org/10.1144/geochem2013-213

Liu JC, Wang YT, Huang SK, Wei R, Sun ZH, Hu QQ, Hao JL (2020) The gold occurrence in pyrite and Te-Bi mineralogy of the Fancha gold deposit, Xiaoqinling gold field, southern margin of the North China Craton: implication for ore genesis. Geol J. 55:5791–5811 https://doi.org/10.1002/gj.3637

Livach AE, Churavtsov AP, Tretyakova NI (2007a) Russian federation state geological map of 1:200,000 Scale, 2 edn. Sugoy Series. Sheet P-56-XII (Ayaks). Explanatory Note. VSEGEI, Saint Petersburg (**in Russian**)

Livach AE, Churavtsov AP, Tretyakova NI (2007b) Russian federation state geological map of 1:200,000 Scale, 2 edn. Sugoy Series. Sheet P-56-XVIII (Omsukchan). Explanatory Note. VSEGEI, Saint Petersburg (**in Russian**)

Livach AE, Tretyakova NI (2022) Balygychan-Sugoy continental rift: structure, basic development features, and metallogeny. Bull North-East Sci Cent FEB RAS 2:3–13. https://doi.org/10.34078/1814-0998-2022-2-3-13(**in Russian with English abstract**)

Makshakov AS, Kravtsova RG (2018) Bryolithochemical studies in the search for and evaluation of gold–silver mineralization based on stream sediments (Northeastern Russia). Russ Geol Geophys. 59:1469–1481 https://doi.org/10.1016/j.rgg.2018.10.007

Makshakov AS, Kravtsova RG (2021) Stream sediments of the Pestrinsk silver-bearing system (Northeastern Russia). Minerals. 11:65 https://doi.org/10.3390/min11010065

Makshakov AS, Kravtsova RG, Tatarinov VV (2019) Lithochemical stream sediments of the Dukat gold–silver ore-forming system (North–East of Russia). Minerals. 9:789 https://doi.org/10.3390/min9120789

Marques ED, Castro CC, de Assis BR, Lombello JC, de Souza MM, Araújo JCS, Santos EAM (2023) Geochemical mapping by stream sediments of the NW portion of Quadrilátero Ferrífero, Brazil: application of the exploratory data analysis (EDA) and a proposal for generation of new gold targets in Pitangui gold district. J Geochem Explor. 250:107232 https://doi.org/10.1016/j.gexplo.2023.107232

Melo G, Fletcher WK (1999) Dispersion of gold and associated elements in stream sediments under semi-arid conditions, northeast Brazil. J Geochem Explor. 67:235–243 https://doi.org/10.1016/S0375-6742(99)00053-9

Morishita Y, Shimada N, Shimada K (2008) Invisible gold and arsenic in pyrite from the high-grade Hishikari gold deposit, Japan. Appl Surf Sci. 255:1451–1454 https://doi.org/10.1016/j.apsusc.2008.05.131

Morishita Y, Shimada N, Shimada K (2018) Invisible gold in arsenian pyrite from the high-grade Hishikari gold deposit, Japan: significance of variation and distribution of Au/As ratios in pyrite. Ore Geol Rev. 95:79–93 https://doi.org/10.1016/j.oregeorev.2018.02.029

Naseem S, Sheikh SA, Qadeeruddin M, Shirin K (2002) Geochemical stream sediment survey in Winder Valley, Balochistan, Pakistan. J Geochem Explor. 76:1–12 https://doi.org/10.1016/S0375-6742(02)00201-7

Nude PM, Arhin E (2009) Overbank sediments as appropriate geochemical sample media in regional stream sediment surveys for gold exploration in the savannah regions of northern Ghana. J Geochem Explor. 103:50–56 https://doi.org/10.1016/j.gexplo.2009.06.005

Ohta A, Imai N, Terashima S, Tachibana Y (2005) Influence of surface geology and mineral deposits on the spatial distributions of elements concentrations in the stream sediments of Hokkaido, Japan. J Geochem Explor. 86:86–103 https://doi.org/10.1016/j.gexplo.2005.04.002

Palenik CS, Utsunomiya S, Reich M, Kesler SE, Wang L, Ewing RC (2004) "Invisible" gold revealed: direct imaging of gold nanoparticules in a Carlin-type deposit. Am Miner. 89:1359–1366 https://doi.org/10.2138/am-2004-1002

Pals DW, Spry PG, Chryssoulis S (2003) Invisible gold and tellurium in arsenic-rich pyrite from the Emperor gold deposit, Fiji:

implications for gold distribution and deposition. Econ Geol. 98:479–493 https://doi.org/10.2113/gsecongeo.98.3.479
Plyashkevich AA (2002) Mineralogy and geochemistry of North-East Russian tin-silver polymetallic deposits. NEISRI FEB RAS, Magadan (**in Russian**)
Polikarpochkin VV (1963) Geochemical methods for ore deposit prospecting on stream sediments. Sov Geol. 4:63–76 (**in Russian**)
Polikarpochkin VV (1976) Secondary Halos and stream sediments. Nauka, Novosibirsk (**in Russian**)
Raykhbaum YaD (1976) Emission spectral analysis in geochemistry. Nauka, Novosibirsk (**in Russian**)
Rodnov YuN, Zaytsev VI (1985) Correlation of tin and silver mineralization in the Balygychan-Sugoy district of the North-East of the USSR. Magmatism of ore regions of the Far East. Far East Scientific Center of the USSR Academy of Sciences, Vladivostok, pp 155–167 (**in Russian**)
Rogozhin AA (2016) Gold determination in rocks, ores and their processed products by extraction-atomic-absorption method with organic sulphides. NSAM No 231-S. VIMS, Moscow (**in Russian**)
Romanov VA (2008) Stream sediments: theory, methodology and practice. Ways of further development. Otechestvennaya Geol. 1:78–82 (**in Russian**)
Savva NE (2018) Mineralogy of silver in the North-East of Russia. Triumph, Moscow. https://doi.org/10.32986/978-5-89392-823-5-1-544 (**in Russian**)
Savva NE, Volkov AV, Lyubimtseva NG, Prokofiev VYu, Sidorov AA, Murashov KYu, Sidorova NV (2021) Gol'tsovoe Ag–Pb–Zn deposit (Northeastern Russia): geological setting, mineralogy, geochemistry, and ore formation conditions. Geol Ore Depos. 63:185–211 https://doi.org/10.1134/S1075701521030065
Shahrestani S, Mokhtari AR, Hosseini-Dinani H (2018) How does sampling density affect mineralization detection in stream sediment geochemical exploration? A case study from NW of Iran. Geochem Explor Environ Anal. 18:196–203 https://doi.org/10.1144/geochem2017-076
Shahrestani S, Mokhtari AR, Carranza EJM, Hosseini-Dinani H (2019) Comparison of efficiency of techniques for delineating uni-element anomalies from stream sediment geochemical landscapes. J Geochem Explor. 197:184–198 https://doi.org/10.1016/j.gexplo.2018.12.001
Shilo NA, Sakharova MS, Krivitskaya NN, Riakhovskaya SK, Bryzgalov IA (1992) Mineralogy and origin features of gold–silver ores of the north–east part of Pacific Ocean frame. Nauka, Moscow (**in Russian**)
Sidorov AA, Volkov AV, Belyi VF, Alekseev VYu, Kolova EE (2009) The gold–silver Okhotsk-Chukotka volcanic belt. Geol Ore Depos. 51:441–455 https://doi.org/10.1134/S1075701509060026
Sidorov AA, Chekhov AD, Volkov AV, Alekseev VYu (2011) Metallogeny of the inner and outer zones of the Okhotsk-Chukotsk volcanogenic belt. Dokl Earth Sci. 439:949–954 https://doi.org/10.1134/S1028334X11060122
Simmonds V, Jahangiryar F, Moazzen M, Ravaghi A (2016) Investigation on the distribution of gold across the Ahar Area (NW Iran) using stream-sediment and BLEG methods. Resour Geol. 66:213–225 https://doi.org/10.1111/rge.12098
Simon G, Kesler SE, Chryssoulis S (1999) Geochemistry and textures of gold-bearing arsenian pyrite, Twin Creeks, Nevada: implication for deposition of gold in Carlin-type deposits. Econ Geol. 94:405–421 https://doi.org/10.2113/gsecongeo.94.3.405
Sokolov SV (2010) The prediction and estimation of resource potential ore fields, nodes and areas of stray flux on the stages of a regional study of subsurface. Razved Ohr Nedr. 5:48–53 (**in Russian**)
Solovov AP (1959) Theoretical and experimental principles of metallometric surveys. Academy of Sciences of the Kazakh SSR, Alma-Ata (**in Russian**)
Strahler AN (1952) Hypsometric (area-altitude) analysis of erosional topography. GSA Bull. 63:1117–1142 https://doi.org/10.1130/0016-7606(1952)63[1117:HAAOET]2.0.CO;2
Strahler AN (1957) Quantitative analysis of watershed geomorphology. Eos Trans Am Geophys Union. 38:913–920 https://doi.org/10.1029/TR038i006p00913
Struzhkov SF, Konstantinov MM (2005) The metallogeny of gold and silver in the Okhotsk-Chuckchee volcanogenic belt. Nauchny mir, Moscow (**in Russian**)
Tauson LV, Kravtsova RG, Zakharov MN (1990) Petrogeochemical factors affecting the distribution of ore fields in rare-metal ore-magmatic systems (in the Soviet Northeast). Trans (dokl) USSR Acad Sci Earth Sci Sect. 313:286–290
Tauson VL, Kravtsova RG, Smagunov NV, Spiridonov AM, Grebenshchikova VI, Budyak AE (2014) Structurally and superficially bound gold in pyrite from deposits of different genetic types. Russ Geol Geophys. 55:273–289 https://doi.org/10.1016/j.rgg.2014.01.011
Taylor SR (1964) Trace element abundances and the chondritic Earth model. Geochim Cosmochim Acta. 28:1989–1998 https://doi.org/10.1016/0016-7037(64)90142-5
Thomas HV, Large RR, Bull SW, Maslennikov V, Berry RF, Fraser R, Froud S, Moye R (2011) Pyrite and pyrrhotite textures and composition in sediments, laminated quartz veins, and reefs at Bendigo gold mine, Australia: insights for ore genesis. Econ Geol. 106:1–31 https://doi.org/10.2113/econgeo.106.1.1
Torgov VG, Khlebnikova AA (1977) Atomic-absorption determination of gold in a flame and by means of a flameless graphite atomizer after preliminary extraction separation with petroleum sulfides. J Anal Chem USSR. 32:753–757
Umitbaev RB (1986) Okhotsk-Chaun metallogenic province. Nauka, Moscow (**in Russian**)
Vasileva IE, Shabanova EV (2012) Arc atomic-emission analysis in geochemical research. Zavod Lab Diagn Mater. 78:14–24 (**in Russian**)
Vinogradov AP (1962) Average contents of chemical elements in the principal types of igneous rocks of the Earth's crust. Geochemistry. 7:641–664
Volkov AV, Sidorov AA, Prokofiev VY, Savva NE, Kolova EE, Murashov KY (2018) Epithermal mineralization in the Okhotsk-Chukchi volcano-plutonic belt. J Volcanolog Seismol. 12:359–378 https://doi.org/10.1134/S0742046318060088
Wang HC, Yuan ZX, Cheng QM, Zhang SY, Sadeghi B (2022) Geochemical anomaly definition using stream sediments landscape modeling. Ore Geol Rev. 142:104715 https://doi.org/10.1016/j.oregeorev.2022.104715
Wells JD, Mullens TE (1973) Gold-bearing arsenian pyrite determined by microprobe analysis, Cortez and Carlin gold mines, Nevada. Econ Geol. 68:187–201 https://doi.org/10.2113/gsecongeo.68.2.187
Yilmaz H, Sonmez FN, Carranza EJM (2015) Discovery of Au–Ag mineralization by stream sediment and soil geochemical exploration in metamorphic terrain in western Turkey. J Geochem Explor. 158:55–73 https://doi.org/10.1016/j.gexplo.2015.07.003
Yilmaz H, Cohen DR, Sonmez FN (2017) Comparison between the effectiveness of regional BLEG and −80# stream sediment geochemistry in detection of precious and base metal mineral deposits in Western Turkey. J Geochem Explor. 181:69–80 https://doi.org/10.1016/j.gexplo.2017.07.003
Yilmaz H, Yousefi M, Parsa M, Sonmez FN, Maghsoodi A (2019) Singularity mapping of bulk leach extractable gold and –80# stream sediment geochemical data in recognition of gold and base metal mineralization footprints in Biga Peninsula South, Turkey. J Afr Earth Sci. 153:156–172 https://doi.org/10.1016/j.jafrearsci.2019.02.015

Yilmaz H, Ghezelbash R, Cohen DR, Sari R, Sonmez FN, Maghsoudi A (2020) Comparison between the geochemical response of BLEG and fine fraction stream sediments to mineralization in the Eastern Black Sea region, Turkey. J Geochem Explor. 217:106609 https://doi.org/10.1016/j.gexplo.2020.106609

Yilmaz H, Sadeghi B, Cohen D (2022) The efficiency of fractal techniques in geochemical anomaly delineation within BLEG and <180 µm stream sediments in Western Turkey. J Geochem Explor. 236:106957 https://doi.org/10.1016/j.gexplo.2022.106957

Yousefi M, Carranza EJM, Kamkar-Rouhani A (2013) Weighted drainage catchment basin mapping of geochemical anomalies using stream sediment data for mineral potential modeling. J Geochem Explor. 128:88–96 https://doi.org/10.1016/j.gexplo.2013.01.013

Zhang Y, Zhou YZ, Wang LF, Wang ZH, He JG, An YF, Li HZ, Zeng CY, Liang J, Lu WC, Gao L (2013) Mineralization-related geochemical anomalies derived from stream sediment geochemical data using multifractal analysis in Pangxidong area of Qinzhou-Hangzhou tectonic joint belt, Guangdong Province, China. J Cent South Univ. 20:184–192 https://doi.org/10.1007/s11771-013-1475-1

Zhang B, Li N, Shu SP, Wang W, Yu J, Chen X, Ye T, Chen YJ (2018) Textural and compositional evolution of Au-hosting Fe-S-As minerals at the Axi epithermal gold deposit, Western Tianshan, NW China. Ore Geol Rev. 100:31–50 https://doi.org/10.1016/j.oregeorev.2017.08.002

Zhang ZC, Wang YW, He JY, Li DD, Qiu HC, Liu FX, Lai CK (2022) Geology, pyrite geochemistry and metallogenic mechanism of the Wulong Gold Deposit in Liaodong Peninsula. North China Craton Miner. 12:1551 https://doi.org/10.3390/min12121551

Zuo RG (2014) Identification of geochemical anomalies associated with mineralization in the Fanshan district, Fujian, China. J Geochem Explor. 139:170–176 https://doi.org/10.1016/j.gexplo.2013.08.013